Low albedo surfaces and eolian sediment: Mars Orbiter Camera views of western Arabia Terra craters and wind streaks

Kenneth S. Edgett
Malin Space Science Systems, Inc.,
P.O. Box 910148
San Diego, California 92191-0148
edgett@msss.com
Phone: (858) 552-2650 x500
Fax: (858) 458-0503

submitted to *Journal of Geophysical Research—Planets*
July 18, 2001

Suggested Running Head: Mars Dark Eolian Sediment

Abstract. High spatial resolution (1.5 to 12 m/pixel) Mars Global Surveyor Mars Orbiter Camera images obtained September 1997 through June 2001 indicate that the large, dark wind streaks of western Arabia Terra each originate at a barchan dune field on a crater floor. The streaks consist of a relatively thin coating of sediment deflated from the dune fields and their vicinity. This sediment drapes a previous mantle that more thickly covers nearly all of western Arabia Terra. No dunes or eolian bedforms are found within the dark wind streaks, nor do any of the intracrater dunes climb up crater walls to provide sand to the wind streaks. The relations between dunes, wind streak, and subjacent terrain imply that dark-toned grains finer than those which comprise the dunes are lifted into suspension and carried out of the craters to be deposited on the adjacent terrain. Such grains are most likely in the silt size range (3.9–62.5 μm). The streaks change in terms of extent, relative albedo, and surface pattern over periods measured in years, but very little evidence for recent eolian activity (dust plumes, storms, dune movement) has been observed.

Introduction

High spatial-resolution (1.5–6.0 m/pixel) pictures of the Martian surface obtained by the Mars Global Surveyor (MGS) Mars Orbiter Camera (MOC) were used to test models for the origin of large, low-albedo wind streaks in western Arabia Terra, Mars. Figure 1 provides a regional view of the streaks; they typically originate at a dark spot on the southern floor of an

impact crater of 30–170 km diameter, have bright margins, and extend tens to a few hundred kilometers southeast or southwest. The streaks are large enough to be seen from Earth-orbiting telescopes [*NASA and Hubble Heritage Team*, 2001] and have drawn the attention of more than a dozen scientific investigations spanning four decades [*Sagan et al.*, 1972, 1973; *Arvidson*, 1974; *Soderblom et al.*, 1978; *Thomas and Veverka*, 1979, 1986; *Thomas et al.*, 1981; *Peterfreund*, 1981; *Kieffer et al.*, 1981; *Thomas*, 1984; *Presley*, 1986; *McEwen*, 1987; *Presley and Arvidson*, 1988; *Henry and Zimbelman*, 1988; *Strickland*, 1989; *Arvidson et al.*, 1989; *Mustard*, 1997; *Cooper and Mustard*, 1998; *Edgett and Malin*, 2000; *Wyatt et al.*, 2001]. The large, dark streaks are almost unique to western Arabia, a few similar features occur in neighboring Xanthe Terra and in the opposite hemisphere near Marte Valles and the Tartarus Colles [*Thomas et al.*, 1981; *Peterfreund*, 1981; *Zimbelman*, 1986].

The global issue considered here is the physical and sedimentological character of a specific suite low-albedo surfaces and materials on Mars. Knowledge of these issues feeds back upon our collective ability to interpret remote sensing observations and select regions for future, more detailed study on the Martian surface. For example, based upon what was known about these wind streaks back in 1994, the dark streak emergent from Trouvelot Crater of western Arabia was considered for a time as a second choice (after Ares Vallis) for the 1997 Mars Pathfinder landing [*Golombek et al.*, 1997]. Additionally, as observed recently by *Wyatt et al.* [2001],

knowledge of the physical nature of the dark spots and streaks in western Arabia is important because they are among those surfaces that provide some of the best thermal infrared spectral signatures (i.e., strongest absorption features) for interpretation of the planet's upper crust mineralogy, lithology, and eolian transport/sorting processes. At present, remote infrared observations of Mars are the primary means for determining surface mineralogy from orbit, as indicated by the use of a Thermal Infrared Spectrometer (TES) on MGS [*Christensen et al.*, 2001], and the April 2001 launch of a thermal infrared imaging system on the Mars Odyssey orbiter [*Christensen et al.*, 1999].

Analysis of the first MOC narrow angle (NA) camera image of one of the western Arabia wind streaks (picture AB1-03001), suggested that it formed by deposition of silt from airborne plumes of material deflated from dunes located in the crater at the upwind end of the streak [*Edgett and Malin*, 2000]. Saltating sand, as occurs in eolian dunes on both Earth and Mars [*Edgett and Christensen*, 1991], is an effective mechanism for launching the otherwise more cohesive (and thus more resistant to entrainment) silt- and clay-sized particles into suspension [e.g., *Pye*, 1995; *Houser and Nickling*, 2001]. When saltating sand impacts a sufficient supply of loose or crusted silt/clay (as in deflation hollows and playa surfaces), plumes of dust can be raised and carried in suspension for tens to hundreds of kilometers downwind; some examples include those observed in satellite photographs of the Great Sand Dunes of Colorado (Figure 2),

Owens (Dry) Lake in California [*Cahill et al.*, 1996], and White Sands, New Mexico [*Gill et al.*, 2000].

The notion that the Martian surface harbors a population of low-albedo material of particle sizes smaller than sand that can be transported in suspension was basically new when proposed by *Edgett and Malin* [2000]. Suspended Martian sediments were typically assumed to be bright dust; the subject of low-albedo silt was not addressed in reviews regarding Martian surface properties and eolian materials by *Christensen and Moore* [1992] or *Greeley et al.* [1992]. A few prior observations hinted that silt-sized (or finer) dark material might exist [*Dollfus and Deschamps,* 1986; *McEwen*, 1992; *Dollfus et al.*, 1993; *Herkenhoff and Vasavada*, 1999]. *Edgett and Malin* [2000] and *Malin and Edgett* [2001] further described examples throughout large regions of low Martian albedo (i.e., broadband phase-corrected reflectance in visible and near-infrared < 15%), such as Sinus Sabaeus and Syrtis Major, that are thickly-mantled by materials that they interpreted were deposited from suspension. Subsequent MOC images have highlighted the full range of features that contribute to the properties of low albedo regions; including sand dunes, smooth-surfaced sand sheets, smooth-surfaced and in some places cracked coverings (mantles) that drape rugged, pre-existing relief, dark ridge- and mesa-forming units associated with lighter-toned layer outcrops, and bedrock substrates exposed on volcanic surfaces between sand dunes (Figure 3).

Background

General Characteristics and Setting

Martian wind streaks have been used for nearly a third of a century as tools to decipher wind circulation patterns, test general circulation models, compare ground truth at landing sites, and monitor changes in the geomorphic expression of surface materials over short (weeks to years) time scales [*Sagan et al.*, 1972, 1973; *Veverka et al.*, 1977; *Ward et al.*, 1985; *Greeley et al.*, 1974a, 1993, 2000]. Western Arabia stands out as somewhat different from other parts of Mars because of its large, prominent wind streaks, and because the region includes all three of the basic Martian surface color "units" identified from Viking orbiter and telescopic views (Figure 1): "bright red," "dark red," and "dark gray" [*Soderblom et al.*, 1978; *Kieffer et al.*, 1981; *McCord et al.*, 1982; *Presley and Arvidson*, 1988; *McEwen*, 1989; *Arvidson et al.*, 1989]. In terms of albedo, the three units are "bright," "intermediate," and "dark" relative to the average Martian surface, respectively. For example, from the map by *Christensen* [1988], Viking Infrared Thermal Mapper (IRTM) albedo observations (covering a broad band 0.3–3.0 μm) place their reflectance in the range 0.27–0.30 for bright red, 0.22–0.24 for dark red, and 0.14–0.17 for dark gray.

By combining infrared and visible observations made from the Viking IRTM and visible imaging systems, a general view of western Arabia's surface materials emerged in which the bright red surfaces were interpreted to consist of loose, bright dust; the dark red surfaces were suspected of being older, immobile deposits of crusted dust; and the dark gray surfaces were seen as places of active sand transport and/or bright dust removal [*Presley and Arvidson*, 1988; *Arvidson et al.*, 1989; *Christensen and Moore*, 1992]. Variants on this interpretation included the possibility that dark red surfaces are not necessarily crusted, but are rougher than bright red surfaces (providing more shadows) at meter scale [*Singer et al.*, 1984]; and that the bright red margins of the large streaks resulted from erosional exposure [*Kieffer et al.*, 1981] or chemical alteration of dark red crusted materials [*Mustard*, 1997].

The color, albedo, and thermophysical units of western Arabia were interpreted as "de-coupled" from underlying bedrock, craters, and other landforms [*Zimbelman and Kieffer*, 1979; *Arvidson et al.*, 1989; *Christensen and Moore*, 1992]. The intercrater plains of the region have been eroded and degraded such that there is an abundance (relative to other heavily cratered plains on Mars) of yardangs and remnant buttes and mesas of layered bedrock [*Presley*, 1986; *Edgett and Parker*, 1997]. This observation was also reflected in the map units of *Greeley and Guest* [1987] and *Scott and Tanaka* [1986]. A relative lack of small valley networks throughout western Arabia was seen as an indication that valley networks were never formed there [*Edgett*

and Parker, 1997] or that erosion long ago removed evidence of ancient valleys [*Hynek and Phillips,* 2001]. Some of the large craters in western Arabia Terra were known to contain buttes and mesas of light-toned material that, at least in the case of Becquerel Crater (located at 22.2° N, 8.1° W), were interpreted to be layered [*Thomas*, 1984]. Subsequent MOC observations have revealed that many of the western Arabia craters contain eroded, exposed, light-toned, layered rock units [*Malin and Edgett*, 2000, 2001].

Deflation Model

Wind streak formation involves all three modes of sediment transport—saltation, traction, and suspension—and a range of particle sizes from clay to pebbles. A variety of wind streak forms have been modeled in wind tunnels and examined in the field on Earth [*Greeley et al.*, 1974a, b; *Maxwell and El-Baz,* 1982; *Greeley*, 1986; *Greeley et al.*, 1989; *Zimbelman and Williams*, 1996]. Wind streaks are recognized because their albedo (or roughness, if observed with radar) is somewhat different than that of their surroundings. This contrast is a direct result of some combination of eolian erosion and/or deposition. Recognition of a wind streak implies that the surface of the streak is physically different than the surface surrounding the streak—the differences can be related to particle size, composition, color, the presence of eolian bedforms, and/or vegetation.

Removal by wind of bright Martian dust was invoked to explain a variety of dark-toned Martian surface features, particularly those that changed and/or formed on time scales of days, weeks, and months over the course of the Mariner 9 and Viking missions [e.g., *Sagan et al.*, 1973; *Veverka et al.*, 1977; *Veverka and Thomas*, 1979]. Perhaps taking a cue from these observations and from the wind tunnel studies of *Greeley et al.* [1974a, b], *Soderblom et al.* [1978] and *Kieffer et al.* [1981] proposed models for the dark streaks of west Arabia Terra that involved eolian deflation to expose a dark substrate. Both groups suggested that wind had eroded down through a surface covered by the dark red unit that pervades the region, exposing a stratigraphically lower dark gray unit. The bright red margins around each dark streak were proposed by *Soderblom et al.* [1978] to be a later mantle of dust superposed on—and maybe trapped along what they proposed to be a rugged, eroded contact between—the dark red and dark gray units. *Kieffer et al.* [1981], on the other hand, suggested that the bright red margins represent a layer of dust that was exposed by deflation because it was stratigraphically sandwiched between the upper, dark red unit, and the lower, dark gray unit.

Saltation Deposition Model

Eolian deflation of sand from the dark intracrater features at the upwind end of each western Arabia wind streak was invoked to explain their genesis. Sand deposition and transfer through a region can create wind streaks, tails, and streamers on Earth [e.g., *Maxwell and El-Baz*, 1982;

Greeley et al., 1989; *Zimbelman et al.*, 1995]. The dark intracrater features of western Arabia were observed in early Viking IRTM data analyses to have thermal properties consistent with the presence of very coarse sand [*Christensen and Kieffer*, 1979]; subsequent studies noted the presence of dunes in some of these craters and proposed that the dark streaks might result from deflation of finer sands, leaving coarser dunes and lag materials on the crater floors [*Thomas et al.*, 1981; *Christensen*, 1983; *Presley*, 1986; *Edgett*, 1995; *Mustard*, 1997]. High spatial resolution thermal inertia studies of the western Arabia streaks [*Henry and Zimbelman*, 1988] and the Pettit Crater streak near Marte Valles by *Zimbelman* [1986] and *Mellon et al.* [2000, p. 451] also concluded that the wind streaks involve saltation transport of fine sand. This model was invoked to explain the bright margins around some of the larger wind streaks: it was suggested that saltating sand mobilizes bright dust and redeposits this material along the margins of the wind streak [*Thomas et al.*, 1981, p. 145]; alternatively, *Mustard* [1997] and *Cooper and Mustard* [1998] suggested that the bright margins were created as saltating sand impinged upon a crusted dust/soil along the margins of the streak.

In the saltation deposition model, it is possible that sands could fine downwind toward the margins of each streak [*Thomas et al.*, 1981]. Fining downwind could occur by eolian sorting, attrition ('kamikaze effect' of *Sagan et al.* [1977]), or both. In this model it is possible to consider that the length of each streak is dictated by the distance a grain of sand can travel from

an intracrater dune field to a location downwind before it has comminuted to silt- and clay-sized particles that are removed in suspension. Alternatively, the sand might not fine downwind, especially if composed of hard, durable material; if this were the case, then accumulations of sand in the form of drifts and/or dunes along the outer streak margins would be expected, just as active burning occurs along the margins of a wind-stoked brush fire.

Suspension Deposition Model

Thomas and Veverka [1979] and *Thomas et al.* [1981] noted a lack of dunes within the western Arabia wind streaks—at least to the limit of Viking and Mariner 9 image resolutions available for the area (typically 100–250 m/pixel). *Thomas and Veverka* [1979, p. 8143] further noted that the streaks appeared to be relatively thin features because of their time-variability between Mariner 6 and Viking 2, and that the dark material "coats hills and flat places alike" as would a granular material deposited from suspension. In their initial study of one of the western Arabia wind streaks in MOC image AB1-03001, *Edgett and Malin* [2000] also found no dunes in the wind streak but an abundance of evidence that the terrain in which the streak occurred was thickly-mantled by smooth-surfaced material that they proposed was deflated from the adjacent crater floor and its attendant dune field. In this model, deflation of fine, dark grains from the intracrater dune fields and/or layered interior materials results in suspension of very fine sand-, silt- and clay-sized particles. The very fine sand and coarser silt grains are just massive enough

that they are not transported very far (a few tens to hundreds of kilometers at most) before falling out of suspension [*Edgett and Christensen*, 1994, p. 2008], while the very finest grains either fall out at the streak margins (providing the observed bright margins) and/or are carried away in long-term suspension.

Approach

Data

The MOC was designed to test specific hypotheses about the nature of Martian geology at the surface/atmosphere interface [*Malin et al.*, 1992]. MOC NA and wide angle (WA) images, acquired between the start of the MGS mission in September 1997 through June 2001, were used to examine the dark streaks in western Arabia Terra. The first MOC picture of a streak in this region, AB1-03001, was acquired early in the MGS orbit insertion phase while the spacecraft was still being aerobraked into its nearly-circular ~380 km-altitude polar mapping orbit. Most (>98%) NA pictures were obtained on nadir-looking passes over surface features of interest. The maximum NA nadir field of view (from the mapping orbit) is 3 km in width and images cover areas of a dozen to several dozen kilometers in length. Pictures of the wind streaks, dark intracrater spots, and surrounding terrain in western Arabia were acquired as opportunities were presented by the coincidence of available downlink, predicted orbital ground track, and the

crossing of critical contacts (e.g., streak margins, transitions from intracrater dark spot to dark streak outside of the crater); most of these opportunities were identified and targeted 1–4 days before the image was obtained. The pictures were usually acquired at spatial resolutions in the range 1.5 to 6 m/pixel to provide a combination of the highest resolution possible (1.5 m/pixel) and longer images of slightly lower resolution but improved signal-to-noise designed to traverse across features of interest at similar solar incidence conditions.

Testing Deflation Model

To use MOC images to look for evidence of deflation as a cause for the western Arabia streaks, one would look for clues (e.g., steep slopes at streak/plains contacts) that the streak surface is topographically lower than the surrounding terrain; one would also look for eolian landforms common to deflation settings. *Malin and Edgett* [2001] observed that diagnostic deflation features at MOC image scales include pedestal craters (formed by ejecta armoring of material otherwise subject to removal by wind), yardangs, and triangular remnants in the "shadow" or lee of decameter-scale obstacles. In the presence of one or more of these features, megaripples and/or granule ripples [*Sharp,* 1963; *Greeley and Iversen,* 1985, p. 154] can also be taken to indicate deflation because these eolian ripples form mostly as lags of granule and pebble-sized clasts piled-up by traction induced by deflating sand. If the layer of material deflated dust was only of a few millimeters or centimeters in thickness, then it would be difficult

to conclude that deflation had taken place using 1.5–6.0 meters/pixel MOC images in the absence of any of the diagnostic landforms.

Testing Saltation Deposition Model

Using a MOC image to look for evidence that sand saltation and deposition contribute to the nature of western Arabia Terra streaks, one would look primarily for dunes, drifts, ripples, and/or thick eolian covers with streamers and swales indicating interaction of the streak material with topographic features in the area (e.g., the patterns of interaction seen in the Ganges Chasma sand sheet in Figure 3b). Deflation of dune sand from an intracrater source would be evident in the form of sand drifts and dunes that 'climb' up out of the crater and 'spill' over onto the terrain outside the crater. Further downwind, dunes and drifts would tend to accumulate at the downwind end of pits and hollows or in the lee of projections or lee-facing scarps. Dunes might be more abundant along streak margins, provided that the sand is not severely comminuted during transport down the length and toward the margins of the streak—alternatively, dunes would be more abundant near the streak's intracrater source if the sand fines to silt downwind. In a zone where sand is moving through the area, deflation could also occur as the sand abrades the subjacent surface *Thomas* [1984, p. 220].

Testing Suspension Deposition Model

MOC image investigation to explore the suspension and deposition model would involve both confirming the absence of forms attributed to saltation and deflation (sand dunes, drifts, ripples, yardangs, pedestal craters, etc.), and the affirmation that the surfaces appear draped by dark streak-forming material. Contacts along the margins of the streaks might reflect this mantling, as well, in which the surfaces adjacent to the streak margins might appear more rugged or more cratered because they have not been covered with the mantling material. Thermophysical observations such as those by the Viking IRTM or MGS TES that suggest the wind streaks consist of sand-sized rather than silt-sized particles [*Presley and Arvidson*, 1988; *Zimbelman*, 1986; *Mellon et al.*, 2000] would not necessarily alter the interpretation that these streaks result from deposition of grains from suspension if (a) the suspended materials were very coarse silt and/or very fine sand [*Edgett and Christensen*, 1994], (b) the streak material is moderately indurated to give the impression that it consists of a coarser particle size, or (c) sufficient patches (1-5 km diameter) of coarser material, including rock outcrops on steep slopes (difficult to mantle from airfall) are present.

Definitions

Particle Sizes

Unless otherwise noted, particle sizes are described in terms of the standard *Wentworth* [1922] sedimentology scale. The exception is the term, "dust," which in Mars scientific literature refers to the very fine-grained materials capable of long-term transport via suspension in the modern Martian atmosphere. The terms "long term suspension" and "short term suspension" are used as described by *Tsoar and Pye* [1987, p. 141-143] and *Edgett and Christensen* [1994, p. 2008] to indicate materials that can be transported aloft over great distances (typically thousands of kilometers) versus those transported at lower altitudes over less than several hundred kilometers. Martian dust particle sizes are < 10 μm and in most cases < 2 μm [*Pollack et al.*, 1995; *Tomasko et al.*, 1999].

Mantles

The term, "mantle," refers to surficial sedimentary deposits of smooth texture (at the pixel scale of 1.5–20 meters) and locally uniform thickness that appear to drape all but the steepest topography. In this sense, a mantle exhibits a morphology similar to that of terrestrial loess and primary air fall tephra deposits. Some mantles observed on Mars are many meters thick [*Zimbelman and Greeley*, 1982; *Schaber*, 1980; *Christensen*, 1986; *Malin and Edgett*, 2001]. Unlike dunes or thick sand sheets, mantles have involved little or no ground transport and

interaction with local topography—i.e., mantles do not have the tails or depressions that arise in the lee of obstacles in an environment of transport by saltation and traction. For comparison, Figure 3b shows an example of the latter—a thick, low albedo sand sheet on the floor of Ganges Chasma—in which the sedimentary material has created moats and streaks via wind interaction with small topographic obstacles, and Figure 3c has an example of a mantled surface.

Tone and Albedo

The terms "dark-toned" and "light-toned" refer to the relative albedo of features in MOC NA images. The NA data are not calibrated so as to provide a quantitative measure of albedo, and all of the grayscale images presented have been contrast-enhanced to emphasize geologic and geomorphic detail unless otherwise noted. The term "albedo" is used in a similar relative sense, unless otherwise noted to have a quantity. For simplicity, all albedo quantities herein come from the peer-reviewed, published 2° x 2° near-global maps derived from Viking IRTM observations by *Christensen* [1988].

MOC Image Identification

MOC images are identified using the convention described by *Edgett and Malin* [2000] and *Malin and Edgett* [2001], in which a three character prefix indicating a specific MGS mission subphase is followed by a hyphen and a five-digit number specifying an image acquired during

that subphase. For example, image M07-03968 was the 3968th picture obtained during the seventh month of the MGS primary mapping mission, and image E05-01291 was the 1291st image acquired in the fifth month of the MGS extended mission. Most MOC images, especially the NA pictures, are much too large to be displayed in their entirety on a printed journal page. For this reason, the MOC images presented here, with the exception of some MOC context views, are sub-frames of the original image.

Observations and Interpretations

Organization

The first step in testing the models for dark wind streak formation was to examine all of the NA images to document the natures of the streaks, intracrater dark spots, other intracrater surfaces, and the surrounding terrain. From this effort, an example of characteristics common to all of the streaks emerged. Observations and interpretations of the type example are presented first, followed by a more detailed account of the observations of the streaks, their associated features, and evidence for eolian activity throughout the region.

Type Example

Examination of all MOC images of western Arabia Terra wind streaks led to selection of one emanating from an impact crater at 10.9°N, 347.8°W, as "typical" because it shares the basic attributes of all of the streaks in the region. Figure 4a shows that MOC NA views cover portions of the crater floor and dark streak associated with the crater; two of these NA images overlap allowing an opportunity to look for changes that occurred in the interval between acquisition of the two images. Figures 4b–e sample the surfaces of the dark intracrater feature and dark wind streak along a single NA image, allowing comparison under similar illumination and atmospheric conditions.

The dark feature in the crater at 10.9°N, 347.8°W is a dune field (Figure 4b). The dunes are barchans, their slip faces are on the south side of each dune, and a few have horns on their east sides that extend somewhat farther southward than the horns on their west sides. The dune orientation confirms that sand has been transported from north toward south, the same direction inferred from the location and orientation of the wind streak outside the crater (Figure 4a). The dune field was photographed twice, first in September 1999 (Figure 4g) and again in September 2000 (Figure 4h). The dunes do not appear at this scale (6 m/pixel) to have changed during the 0.55 Mars year interval between the two pictures. No other changes, such as avalanches on the dune slip faces, were observed.

The dune field does not extend all the way to the south crater wall, nor do any dunes climb this wall. The area in Figure 4b is the main concentration of dunes in the crater; about 9 km of dune-free space occurs between the dune field and the southern crater floor/wall interface toward which the dunes are or were advancing. As sand-sized particles are most likely to be the principal sediment within Martian dunes [*Cutts and Smith*, 1973; *Edgett and Christensen*, 1991, 1994], these relations indicate that the amount of sand-sized material available for transport within the crater at 10.9°N, 347.8°W, is fairly limited. Barchan dunes are usually considered to be a variety common to areas of "low sand supply" or where sand is merely being passed through the area [*Wasson and Hyde*, 1983; *Lancaster*, 1989, pp. 2–6]. That the dunes have not reached the south crater wall and piled up (or climbed the crater wall) suggests that the sand is a relatively recent addition to the area (how recent depends upon where it originated and how fast the dunes are moving). That the slip faces indicate southward movement indicates that slope winds coming northward off the south crater wall, if they occur at all, are not strong enough to deflect the dunes or re-shape them at their present distance from this wall.

The dark wind streak begins within the dune field. Figure 4i shows two dunes trapped in a crater north of the main dune field shown in Figures 4b, 4g, and 4h. A dark surface widens outward and southward from these two trapped dunes, this surface mantles underlying light-

toned ripple-like ridges that occur in depressions all around this dark area (labeled "deflated material(?)" in Figure 4i). The configuration of the two trapped dunes and the dark streak suggest deflation of dark material from the dunes and subsequent settling of this material on the subjacent downwind terrain; a similar situation is inferred from dunes in another western Arabia Terra crater in Figure 5. Further south, beyond the main body of dunes, the crater wall is similarly mantled by dark-surfaced material (Figure 4c). The mantle on the south crater wall is smooth at the 6 m/pixel scale of the MOC image. Smooth material drapes all but the steepest ridges near the crater rim at the south end of Figure 4c. The wall material is not as dark as the dune and interdune surfaces in Figure 4b, but the dark surface at the northeast (upper right) corner of Figure 4c indicates that there is an abrupt change in relative albedo at the floor/wall interface. Outside the crater, the dark wind streak surface also appears smooth; examples from the middle and southern margin of the streak are in Figures 4d and 4e, respectively. No dunes or ripples occur in the wind streak. In all cases, Figures 4c–e, the surface is mantled such that low areas are filled-in and somewhat flattened, high areas protrude above this smooth material and retain a rugged appearance at meter scales on their steeper slopes, and only a few small impact craters are present.

The overall impression from Figures 4c–e and 4i is that dark material deflated from the dunes, or their vicinity, has been draped over the downwind terrain. In other words, the dark

streak material appears to mantle underlying terrain as if deposited from suspension. For this to occur, the grains comprising the streak would have to be finer than those that compose the dunes; i.e., silt-sized grains (with possible very fine sand at one end and clay-sized grains at the other). The lack of eolian bedforms on the wind streak surface strengthens the suspension argument because there are no landforms that would result from saltation transport. Further enhancing the impression that a mantle is present is MOC image E02-02843, which in Figure 4f crosses the bright margin of a wind streak immediately south of the crater at 10.9°N, 347.8°W. This streak actually emanates from the neighboring impact crater at 11.6°N, 346.7°W. The dark- and lighter-toned surfaces at the streak margin are somewhat different. Both surfaces are smooth at decameter scales but the light-toned surface at the streak margin and the intermediate-toned surface out beyond the margin have irregularly-shaped patches of intermediate-toned material (darker than the terrain beyond the streak margin) ranging in size from a few tens to a few hundred meters across. These patches are not visible in the dark wind streak, though they occur right up to its margin; these observations suggest that the intermediate-toned patches predate and are superposed by the dark streak-forming material. As for the bright streak margin, it is only distinguished from the adjacent terrain beyond the streak margin because it is brighter; there are no sharp albedo nor topographic boundaries separating the dark material, nor the adjacent intermediate-toned plains, from the bright streak margin. These observations indicate that the bright margin may consist only of a thin veneer of bright material (e.g., dust); the intermediate-

toned patches within the bright margin may be physically rougher surfaces such that shadowing causes them to appear darker than the surrounding bright streak margin terrain.

Crater Interiors

Dark-toned Landforms and Surfaces

The typical western Arabia Terra wind streak begins at a dune field on a crater floor and extends downwind as a mantle deposit that drapes underlying terrain (Figure 4). *Thomas* [1984] suspected that all western Arabia dark streaks began at an intracrater dune field; *Edgett and Christensen* [1994] interpreted Viking IRTM observations and the Mariner and Viking images listed in Table 1 to indicate that all of these dune fields would consist of barchans separated by (usually) a coarser interdune substrate. Through June 2001, 116 MOC NA images of dark intracrater features in western Arabia Terra were acquired. These images cover portions of 48 of the 153 total dark intracrater spots in the region, and most that have not been photographed are the smallest (< 10 km wide) dark spots. Table 1 lists the first image acquired by any spacecraft that showed a dune field within 43 of the 48 dark intracrater spots in western Arabia Terra. As with the example in Figure 4, the dune fields consist of barchans located more than a few kilometers north of the southern crater walls, all have slip faces pointed in the same direction indicated by the adjacent dark wind streak. All of the dunes in these craters are dark-toned. In some craters, eolian bedforms smaller and lighter-toned than the dunes are present in isolated

troughs and depressions; in some cases, the darker dunes have over-ridden the lighter-toned bedforms [*Edgett and Malin*, 2000, Figure 24; Malin and Edgett, 2001, Figure 38].

Not all dark intracrater spots exhibit dune fields (Table 2). While the list is short (5 locations), four of the dark intracrater features listed in Table 2 have something in common: they do not have a dark wind streak. The remaining one on the list has a wind streak, but MOC coverage is not adequate to be certain that no dunes are present. An example of a location without a wind streak and without dunes is the dark spot in Curie Crater (Figure 6). Two MOC NA images cover portions of the dark spot in Curie Crater, and neither exhibits dunes although patches of what may be sand can be seen filling small pits and craters. In Curie Crater, perhaps there is insufficient sand to pile up to form dunes; likewise there is insufficient dark material to form a streak downwind of the dark spot. Alternatively, it is possible that dunes are present in Curie Crater, but a picture of them has not yet been acquired; as with some of the others listed in Table 2, the darkest portions of the low albedo feature in Curie has not been photographed.

Some of the dark material on crater floors in western Arabia Terra are not dune fields nor are they like the dark surfaces in Curie Crater. Figure 7 shows a portion of the low albedo surface within Crommelin Crater at 5°N, 11°W; the dark material in this case is a smooth-surfaced steep-sided mesa-forming unit that overlies a rugged, lighter-toned surface seen in

windows through the dark mesa-forming unit. Dark mesa-forming units are most common in craters along the southern margins of the western Arabia Terra region, that is, they are in craters closest to Terra Meridiani. (Figure 8). Indeed, along the northern margins of Terra Meridiani, dark mesa-forming units can be found on the intercrater plains, as well (Figure 9). The rugged appearance of the underlying light-toned units implies that the dark mesa-forming material was emplaced after the light-toned material achieved its rugged appearance (i.e., the dark mesa-forming units lie unconformably upon a previously eroded surface).

Layer Outcrops

Malin and Edgett [2000] identified dark mesa-forming units as a common, unconformable upper geologic unit among sequences of otherwise light-toned layered and massive outcrops found in craters, chasms, chaotic terrain, and intercrater plains throughout equatorial Mars. Light-toned layered outcrops are common on the floors of craters that have wind streaks in western Arabia Terra, though they are more common and more extensive in craters closest to the light-toned layer outcrops of northern Terra Meridiani (Figure 8). Craters farther from Terra Meridiani have smaller layer outcrops, such as the isolated features in Trouvelot and Becquerel craters (Figure 10), and many others away from Terra Meridiani have no such outcrops, such as Curie Crater (Figure 6). The layer units exhibit cliff-bench morphology, preserve faults and fault off-sets, and in most cases are of similar thickness from one layer to the next (Figure 11). Some

layer outcrops appear to be the source of light-toned material that has been shed to form light-toned wind streaks (Figure 12). The morphologic characteristics of the layer outcrops suggest they are indurated materials (e.g., hard like rock); the repeated thicknesses suggest repeated changes in their depositional environment; and the shedding and eolian transport of bright grains suggests their particles sizes are fine (e.g., clay to very fine sand, materials too small to create bedforms). *Malin and Edgett* [2000] hypothesized that the layers formed in intracrater lakes or via atmospheric processes in an early Martian environment very different from the one found today; a lacustrine model was advocated previously for the layer outcrops in Becquerel Crater by *Forsythe and Zimbelman* [1995]. MOC images of the layers in Becquerel Crater show that some of the layers may be dark-toned (Figure 13).

Other Crater Interior Surfaces

Most crater interior surfaces that do not consist of dunes, interdune surfaces, dark mesa-forming units, or light-toned layer outcrops, are smooth at the hectometer scales of Viking and Mariner 9 orbiter images, but rugged and craggy at MOC's decameter scales (Figures 14a, b). In some cases, the rugged and craggy crater floors result from deflation, probably by wind, as indicated for example by the presence of pedestal craters formed by armoring of otherwise deflatable surfaces by crater ejecta (Figure 14c). Other crater interior surfaces, especially crater

walls that are not subjacent to the dark wind streaks of the region, are thickly mantled by materials that have smooth, intermediate-toned surfaces (Figure 14d).

Surrounding Terrain

Surficial Materials

The upper surface material, that which gives western Arabia Terra its distinctive "dark red" color and intermediate albedo [*Presley and Arvidson*, 1988; *Arvidson et al.*, 1989; *Christensen and Moore*, 1992], is a mantle deposit (Figure 15). The mantle is thinner than the mantles on the crater rims (e.g., Figure 14d) and may be no more than a few meters thick (Figure 15). *Christensen and Moore* [1992] predicted on the basis of thermophysical properties that the surface in this region would be mantled; following *Presley and Arvidson* [1988], they predicted that the mantle would be crusted and might represent a stratigraphically older mantle than the higher-albedo material covering most of central Arabia Terra. The stratigraphic position and state of induration of the "dark red"-surfaced mantle in western Arabia Terra are unknown. Except for apparent thickness, the mantle covering the intercrater plains is identical to the material on crater walls and rims throughout the region (Figure 14d).

Substrate and Subsurface Materials

The bedrock beneath the mantle that covers most of western Arabia is layered. Evidence for layering can be seen, for example, in Figures 16 and 17. Erosion that pre-dates the mantling of the region by the dark red-surfaced material has exposed and expressed the regional layered basement as terraces (Figures 16, 17), yardangs (Figure 18), and pedestal craters (Figures 16, 18) [*Presley*, 1986; *Edgett and Parker*, 1997]. In the far western areas around Mawrth Vallis, the bedrock is not mantled and reveals dark mesa-forming units overlying light-toned layered units similar to those in the craters of western Arabia as well as among other light-toned layered outcrops across the surface of Mars [*Malin and Edgett*, 2001]. Along the margins of some wind streaks, such as that which emanates from Rutherford Crater, similar dark mesa-forming units and light-toned substrates are exposed (Figure 19). In the case of the Rutherford streak, the light-toned substrate and dark mesa-forming material do not comprise the entire streak; rather, the material that gives the overall streak its dark tone is a thin veneer superposed on these surfaces.

Streak Surfaces

Variety and Comparison to Viking

Thomas and Veverka [1979] observed that the wind streaks in western Arabia change in terms of length and albedo relative to surrounding terrain on time scales short enough to have been observed between the Mariner 6 (1969), Mariner 9 (1972) and Viking orbiter (1976-1980)

missions. Consistent with this observation, many of the streaks are different in MGS MOC wide angle views than they were when seen by the Viking orbiters. Figure 20 documents four basic types of changes that are observed. Relative to their surroundings, some streaks are about the same as they were during the Viking mission, others became lighter, others disappeared, and others grew longer. Little or no change has occurred during the MGS mission through June 2001.

Dark Streak Surfaces

Edgett and Malin [2000] studied NA image AB1-03001, which shows portions of a crater and dark streak located at 4.2°N, 5.3°W. They concluded that the streak consists of a thick, smooth-surfaced mantle that obscures much of the underlying surface. Subsequent images from the MOC WA cameras, as well as MGS TES visible/near-infrared reflectance measurements (S. W. Ruff, Personal Communication, February 2000), show that the dark streak observed by the Viking orbiters is no longer present (Figure 20c). In fact, the streak was not present on October 29, 1997, when image AB1-03001 was acquired; the lack of the streak early in the MGS mission was indicated by the earliest MOC WA image of the area, AB1-04701, which was obtained a few weeks later on November 18, 1997.

While the dark streak examined by *Edgett and Malin* [2000] turned out not to be present when the AB1-03001 image was acquired, they found that, like the typical streak described

above and in Figure 4, the surface downwind of the dark intracrater dunes is mantled. A mantled surface downwind of the dunes, whether on a dark streak (Figures 20a, d), a light streak (Figure 20b), or a location that formerly had a streak (Figure 20c), is a clear indicator that the surface is not deeply eroded as it might be if the deflation model were to hold for these streaks. The fact that the streak in Figure 20c was missing at the time that image AB1-03001 was acquired suggests that either the dark streak-forming material had been removed, or it had been covered by brighter material. Removal of the dark streak would imply that the streak-forming material is a thin veneer, and that the material beneath this streak was a mantled surface prior to deposition of the streak (and remained such after the streak was removed). Burial of the dark streak would say nothing about the thickness of material comprising the streak, though only a thin veneer of dust with an albedo the same as the surrounding terrain would be required to obscure the streak. Burial would also imply that there could be a complex microstratigraphy within the mantle downwind of the crater, in which alternating layers of dark, intermediate, and perhaps light-toned sediments might be found.

As noted in the type example illustrated in Figure 4, the wind streaks in western Arabia Terra usually have smooth surfaces at decameter scales. In no cases are the streaks composed of dunes. In cases where ripples or ripple-like features are present in the streaks (as observed by *Edgett and Malin* [2000] in the AB1-03001 image), they are mantled and oriented differently

than the wind direction implied by the streak. In a few locations there are superposed on the dark streaks some small (a few kilometers long, at most) bright wind streaks and tails in the lee of smaller craters and obstacles (Figure 21); these streaks and tails indicate that there has been some eolian transport at ground level (perhaps removal of bright dust coatings) that has in some way influenced the dark streaks in which they occur. Some of the dark streaks consist of or are underlain by thick mantles (Figure 4d–f). Other streaks are a veneer so thin that underlying dark and light-toned outcrop materials are revealed along their margins (Figure 19). Figure 22 shows a case in which there is no discernable difference in mantle thickness (nor the population of ridged and pitted surfaces found at this location) between the streak surface and the terrain out beyond the streak, a relationship implying that the dark streak material is a thin covering relative to the scale of a MOC image (i.e., << 1 m).

Eolian Activity

Eolian activity has long been presumed to be the primary cause for changes in western Arabia wind streak albedo, length, and configuration [*Sagan et al.*, 1973; *Veverka and Thomas*, 1979]. Given that these changes are known to occur over periods as short as a few Earth years, other evidence for contemporary eolian activity in western Arabia Terra was sought by looking for changes among the intracrater dune fields and by searching for dust devils and dust plumes in NA and full-resolution WA images acquired through June 2001.

Dust

Dust devils and dust plumes are excellent evidence for present-day eolian activity. If the suspension deposition model for the genesis of the western Arabia Terra wind streaks was the correct model, it would be ideal to see wind blowing such a plume across the landscape, as has been observed on Earth by orbiting spacecraft (Figure 2). Martian dust events can range in size from small plumes of only a few kilometers in scale up to global dust storms. Through June 2001, no global dust storm was observed by MGS, and no dust storms large enough to be spotted by the MOC's 7.5 km/pixel daily global images were detected in western Arabia Terra [*Cantor et al.*, 2001]. Thus, a search for smaller, localized dust events was conducted by examining all of the several hundred NA images and the highest-resolution WA images (~240 m/pixel) of the region. Most of the full-resolution WA images are ~115 km by ~115 km square context views taken at the same time that a NA image was obtained. Other full-resolution WA pictures were acquired during the geodesy campaign in May 1999 [*Caplinger and Malin*, 2001].

Dust devils on Mars were recorded from orbit by the Vikings and both the NA and WA MOC cameras [*Thomas and Gierasch*, 1985; *Malin and Edgett*, 2001]. Full resolution WA images have captured dust devils in a few locations where they are known to grow to sizes large enough to be seen by these cameras; *Malin and Edgett* [2001] noted dust devils of this size in

Amazonis Planitia and Solis Planum in May 1999. It is not known whether similar large dust devils might occur elsewhere, because there have been no global systematic searches of the 240 m/pixel data. None of the WA nor NA images of western Arabia included a dust devil. However, filamentary streaks attributed to the disruption and/or removal of thin surface coatings of dust by the passage of dust devil vortices are observed in NA images of some of the dune fields in western Arabia (Figure 23). In other locations on Mars, dust devils have been caught in the act of creating thin filamentary streaks; the streak patterns can change over intervals of a few months to an Earth year [*Malin and Edgett*, 2001]. It is likely that the streaks in Figure 23 were recent (a few months old at most) features at the times the pictures were acquired.

Dust plumes caused by wind are expected to occur in western Arabia because a Viking orbiter image showed a few dust plumes rising from an intercrater surface just a few tens of kilometers south of the southernmost west Arabia wind streaks (Figure 16) in April 1978. Some clouds connected to large dust storms on the northern plains obscured portions of northwestern Arabia Terra in WA pictures acquired May 8-14, 1999, October 14, 1999, and March 30, 2000 (see images M01-00461, M01-00641, M01-01030, M01-01032, M01-01238, M01-01240, M01-01446, M01-01631, M08-03018, M13-02172, M13-02174), but no dust plumes rising from western Arabia surfaces are found in any of the NA or WA images.

Sand

The lack of observed dust activity in western Arabia may suggest that very little eolian activity (except occasional dust devils that create filamentary streaks, Figure 23) occurred in the region during the MGS mission. Another approach to assessing eolian activity is to check the intracrater dune fields for movement. Smaller dunes, such as barchans of a few to a few tens of meters in planform dimensions, typically mover faster than large dunes [*Gay,* 1999], and thus would be the best candidates to examine for change. As noted above, there is no sign of change in dune position or shape between September 1999 and September 2000 in the dune field portrayed in Figure 4. Likewise, *Malin and Edgett* [2001, Fig. 40] detected no change in a western Arabia dune field over an interval spanning May 1978 (Viking image 709A42) to December 1999 (MOC image M10-02916). Figure 24 shows an additional example from the search for change in dune position, shape, or size; in this case the images compare dunes in 1998 with 2001. In addition to the pairs of images in Figures 4 and 24 and in *Malin and Edgett* [2001, Fig. 40], the following pairs were also examined: (a) SP2-44207 and M04-01484, (b) SP2-40803 and M11-01425, and (c) M07-01459 and E05-02646. No changes in dune position or shape were observed in any cases, nor has any evidence of movement on the dune slip faces (e.g., avalanches) been observed. Change among these dune fields at the present time has been minimal.

Summary and Conclusions

The dark streaks of western Arabia Terra consist of a relatively thin coating of sediment deflated from sand dune fields on their adjacent crater floors. The sediment drapes pre-existing terrain and creates no bedforms that can be observed at MOC image resolutions (1.5 to 12 m/pixel). This conclusion differs from that of *Edgett and Malin* [2000] because it is now recognized that the wind streaks are superposed on a surface that in most places was previously mantled by a thicker, intermediate-toned deposit. This thicker deposit also covers much of western Arabia Terra.

The bright margins of the wind streaks in western Arabia are also a thin coating, probably consisting of ephemeral, loose dust. In terms of Viking color "units" [e.g., *Arvidson et al.*, 1989], "dark red" is the color of the surface of the meter- (or more) thick mantle that unconformably drapes crater walls and the eroded, layered, intercrater terrain; "bright red" surfaces, at least in the context of the dark wind streaks, are veneers of dust; and "dark gray" surfaces include the dark wind streaks, the intracrater dune fields, and dark mesa-forming units.

Most, if not all, dark wind streaks originate at a dune field. The dune slip faces are oriented in the same direction as the wind streak, indicating that the winds that effect the dunes are the same as those that affect the streaks. No dunes are observed on the wind streaks or climbing out

of the craters toward the wind streaks. Eolian physics, dune morphology, and thermal infrared observations all argue that Martian dunes consist of sand [*Cutts and Smith*, 1973; *Edgett and Christensen*, 1991]. Deflation of grains finer than sand, but coarser than the average bright Martian dust, explains the genesis of the western Arabia wind streaks and constrains the particle size of streak-forming materials to the silt and very fine sand size ranges (clay-size grains are subject to long-term suspension and thereby removal from the region [*Edgett and Christensen,* 1994]). Small bright wind streaks that occur within a few of the larger dark streaks (Figure 21) may result from eolian deflation of dust that occasionally settles on dark streak surfaces [e.g., *Greeley et al.,* 1974a, b], though how this dust is mobilized on an otherwise smooth, dust-free surface is unclear.

The wind streaks are subject to change over multiple-year periods, but all streaks do not exhibit the same changes over time; for example, they do not all grow longer or shorter together, nor do they grow darker or brighter together. Brightening of dark streaks and the disappearance of the streak in Figure 20c might occur via deposition of new dust coming out of long term suspension in the atmosphere, or perhaps by deposition of grains derived from erosion of light-toned layer outcrops that occur within the adjacent craters (Figure 12). Despite the evidence for changes in wind streak pattern and extent over multiple-year periods, very little evidence for recent eolian activity in the region was found. Dark filamentary streaks on some dune surfaces

suggest that dust devil vortices may form and move through the region from time to time, but no vigorous wind-induced dust plumes were observed, and there has been no sign of change among the intracrater sand dunes in terms of position, shape, or slip face avalanches. It is very possible that very little eolian activity occurs in this region except during major dust storm events; no dust storms were observed in the region between September 1997 and June 2001.

Craters from which dark streaks emanate typically, though not always, have light-toned layered outcrops within them. These outcrops are more common and cover more crater floor surface area in craters nearest to the layered intercrater terrains of northern Terra Meridiani. Dark mesa-forming units also occur in some craters near Terra Meridiani, but these are generally not abundant and it is unclear whether they contribute sand or silt to the dunes and wind streaks in the region. Crater floors include landforms commonly associated with eolian deflation, such as pedestal craters and megaripples. The dark sand dunes and associated dark wind streaks emanating from these craters may be part of the system by which the layered units in the craters have been eroded and removed from the craters. Some layered units, indeed, exhibit dark layers (Figure 13) that could provide a source for the dark-toned sand dunes and wind streaks.

Acknowledgments

This research was funded by the NASA Mars Data Analysis Program; study of data obtained M19 through E05 was augmented by funds from the Mars Global Surveyor Mars Orbiter Camera experiment.

References

Arvidson, R. E., Wind-blown streaks, splotches, and associated craters on Mars, *Icarus, 21*, 12-27, 1974.

Arvidson, R. E., E. A. Guinness, M. A. Dale-Bannister, J. Adams, M. Smith, P. R. Christensen, and R. B. Singer, Nature and distribution of surficial deposits in Chryse Planitia and Vicinity, Mars, *J. Geophys. Res., 94*, 1573-1587, 1989.

Cahill, T. A., T. E. Gill, J. S. Reid, E. A. Gearhart, and D. A. Gillette, Saltating particles, playa crusts and dust aerosols at Owens (Dry) Lake, California, *Earth Surf. Processes Landforms, 21*, 621-639, 1996.

Cantor, B. A., P. B. James, M. Caplinger, and M. J. Wolff, Martian dust storms: 1999 Mars Orbiter Camera observations, *J. Geophys. Res., 106*, in press, 2001.

Caplinger, M. A., and M. C. Malin, The Mars Orbiter Camera geodesy campaign, *J. Geophys. Res., 106*, in press, 2001.

Christensen, P. R., Eolian intracrater deposits on Mars: Physical properties and global distribution, *Icarus, 56*, 496-518, 1983.

Christensen, P. R., Regional dust deposits on Mars: Physical properties, age, and history, *J. Geophys. Res., 91*, 3533-3545, 1986.

Christensen, P. R., Global albedo variations on Mars: Implications for active aeolian transport, deposition, and erosion, *J. Geophys. Res., 93*, 7611-7624, 1988.

Christensen, P. R., and H. H. Kieffer, Moderate resolution thermal mapping of Mars: The channel terrain around the Chryse basin, *J. Geophys. Res., 84*, 8233-8238, 1979.

Christensen, P.R., and H.J. Moore, The Martian surface layer, in *Mars*, edited by H.H. Kieffer, B.M. Jakosky, C.W. Snyder, and M.S. Matthews, pp. 686-729, Univ. of Arizona Press, Tucson, 1992.

Christensen, P. R., B. M. Jakosky, H. H. Kieffer, M. C. Malin, H. Y. McSween Jr., K. Nealson, G. Mehall, S. Silverman, and S. Ferry, The Thermal Emission Imaging System (THEMIS) instrument for the Mars 2001 orbiter, *Lunar Planet. Sci.* [CD-ROM], *XXX*, abstract 1470, 1999.

Christensen, P. R., J. L. Bandfield, V. E. Hamilton, S. W. Ruff, H. H. Kieffer, T. N. Titus, M. C. Malin, R. V. Morris, M. D. Lane, R. L. Clark, B. M. Jakosky, M. T. Mellon, J. C. Pearl, B. J. Conrath, M. D. Smith, R. T. Clancy, R. O. Kuzmin, T. Roush, G. L. Mehall, N. Gorelick, K.

Bender, K. Murray, S. Dason, E. Greene, S. Silverman, and M. Greenfield, The Mars Global Surveyor Thermal Emission Spectrometer Experiment: Investigation description and surface science results, *J. Geophys. Res.*, *106*, in press, 2001.

Cooper, C. D., and J. F. Mustard, Rates of erosion in Oxia Palus, Mars, *Lunar Planet. Sci.* [CD-ROM], *XXIX*, abstract 1164, 1998.

Cutts, J. A., and R. S. U. Smith, Eolian deposits and dunes on Mars, *J. Geophys. Res., 73*, 4139-4154, 1973.

Dollfus, A., and M. Deschamps, Grain-size determination at the surface of Mars, *Icarus, 67*, 37-50, 1986.

Dollfus, A., M. Deschamps, and J. R. Zimbelman, Soil texture and granulometry at the surface of Mars, *J. Geophys. Res., 98*, 3413-3429, 1993.

Edgett, K. S., Physical properties of the Ares Valles (primary) and Trouvelot Crater (back-up) landing sites for Mars Pathfinder: Thermal inertia and rock abundance from Viking IRTM observations (abstract), *Lunar Planet. Sci., XXVI*, 353-354, 1995.

Edgett, K. S., and P. R. Christensen, The particle size of Martian aeolian dunes, *J. Geophys. Res., 96*, 22,765-22,776, 1991.

Edgett, K. S., and P. R. Christensen, Mars aeolian sand: Regional variations among dark-hued crater floor features, *J. Geophys. Res., 99*, 1997-2018, 1994.

Edgett, K. S., and M. C. Malin, New views of Mars eolian activity, materials, and surface properties: Three vignettes from the Mars Global Surveyor Mars Orbiter Camera, *Journal of Geophysical Research, 105*, 1623-1650, 2000.

Edgett, K. S., and T. J. Parker, Water on early Mars: Possible subaqueous sedimentary deposits covering ancient cratered terrain in western Arabia Terra and Sinus Meridiani, *Geophys. Res. Lett., 24*, 2897-2900, 1997.

Forsythe, R. D., and J. R. Zimbelman, A case for ancient evaporite basins on Mars, *J. Geophys. Res., 100*, 5553-5563, 1995.

Gay, S. P. Jr., Observations regarding the movement of barchan sand dunes in the Nazca to Tanaca area of southern Peru, *Geomorphology, 27*, 279-293, 1999.

Gill, T. E., D. L. Westphal, G. Stephens, and R. E. Peterson, Integrated assessment of regional dust transport from west Texas and New Mexico, Spring 1999, *Proceedings of the 11th Joint Conference on the Applications of Air Pollution Meteorology with the Air and Waste Management Association*, American Meteorological Society, Boston, Massachusetts, pp. 370-375, 2000.

Golombek, M. P., H. J. Moore, and T. J. Parker, Selection of the Mars Pathfinder landing site, *J. Geophys. Res., 102*, 3967-3988, 1997.

Greeley, R., Aeolian landforms: Laboratory simulations and field studies, in *Aeolian Geomorphology*, edited by W.G. Nickling, pp. 195-211, Allen and Unwin, Boston, 1986.

Greeley, R., and J. E. Guest, Geologic map of the eastern equatorial region of Mars, scale 1:15,000,000, *U.S. Geol. Surv. Misc. Inv. Ser. Map I-1802-B*, 1987.

Greeley, R., and J. D. Iversen, *Wind as a Geological Process on Earth, Mars, Venus, and Titan*, Cambridge Univ. Press, 333 p., 1985.

Greeley, R., and J. D. Iversen, Aeolian processes and features at Amboy Lava Field, California, in *Physics of Desertification*, edited by F. El-Baz and M. H. A. Hassan, p. 290-317, Martinus Nijhoff, Dordrecht, 1986.

Greeley, R., J. D. Iversen, J. B. Pollack, N. Udovich and B. White, Wind tunnel studies of Martian aeolian processes, *Proceedings of the Royal Society of London, Series A, 341*, 331-360, 1974a.

Greeley, R., J. D. Iversen, J. B. Pollack, N. Udovich and B. White, Wind tunnel simulations of light and dark streaks on Mars, *Science, 183*, 847-849, 1974b.

Greeley, R., P. Christensen, and R. Carrasco, Shuttle radar images of wind streaks in the Altiplano, Bolivia, *Geology, 17*, 665-668, 1989.

Greeley, R., N. Lancaster, S. Lee, and P. Thomas, Martian aeolian processes, sediments, and features, in *Mars*, edited by H.H. Kieffer, B.M. Jakosky, C.W. Snyder, and M.S. Matthews, pp. 730-766, Univ. of Arizona Press, Tucson, 1992.

Greeley, R., A. Skypeck, and J. B. Pollack, Martian aeolian features and deposits: Comparisons with general circulation model results, *J. Geophys. Res., 98*, 3183-3196, 1993.

Greeley, R., M. D. Kraft, R. O. Kuzmin, and N. T. Bridges, Mars Pathfinder landing site: Evidence for a change in wind regime from lander to orbiter data, *J. Geophys. Res., 105*, 1829-1840, 2000.

Henry, L. Y., and J. R. Zimbelman, Physical properties and aeolian features in the Oxia Palus and Margaritifer Sinus Quadrangles of Mars (abstract), *Lunar and Planetary Science XIX*, 479-480, 1988.

Herkenhoff, K. E., and A. R. Vasavada, Dark material in the polar layered deposits and dunes on Mars, *J. Geophys. Res., 104*, 16,487-16,500, 1999.

Houser, C. A., and W. G. Nickling, The emission and vertical flux of particulate matter <10 μm from a disturbed clay-crusted surface, *Sedimentology, 48*, 255-267, 2001.

Hynek, B. M., and R. J. Phillips, Evidence for extensive denudation of the Martian highlands, *Geology, 29*, 407-410, 2001.

Kieffer, H. H., P. A. Davis, and L. A. Soderblom, Mars' global properties: Maps and applications, *Proc. Lunar Planet. Sci., 12B*, 1395-1417, 1981.

Lancaster, N., *The Namib Sand Sea: Dune forms, processes, and sediments*, 180 p., A.A. Balkema, Brookfield, Vermont, 1989.

Malin, M. C., and K. S. Edgett, Sedimentary rocks of early Mars, *Science, 290*, 1927-1937, 2000.

Malin, M. C., and K. S. Edgett, The Mars Global Surveyor Mars Orbiter Camera: Interplanetary cruise through primary mission, *J. Geophys. Res., 106*, in press, 2001.

Malin, M. C., G. E. Danielson, A. P. Ingersoll, H. Masursky, J. Veverka, M. A. Ravine, and T. A. Soulanille, Mars Observer Camera, *J. Geophys. Res., 97*, 7699-7718, 1992.

Maxwell, T.A., and F. El-Baz, Analogs of Martian eolian features in the western desert of Egypt, in *Desert Landforms of Southwest Egypt: A Basis for Comparison With Mars*, edited by F. El-Baz and T.A. Maxwell, pp. 247-259, NASA CR-3611, 1982.

McCord, T. B., R. B. Singer, B. R. Hawke, J. B. Adams, D. L. Evans, J. W. Head, P. J. Mouginis-Mark, C. M. Pieters, R. L. Huguenin, and S. H. Zisk, Mars: Definition and characterization of global surface units with emphasis on composition, *J. Geophys. Res., 97*, 10,129-10,148, 1982.

McEwen, A. S., Mars as a planet (abstract), *Lunar Planet. Sci., XVIII*, 612-613, 1987.

McEwen, A. S., Temporal variability of the surface and atmosphere of Mars: Viking orbiter color observations (abstract), *Lunar Planet. Sci., XXIII*, 877-878, 1992.

McEwen, A. S., Mars' global color and albedo (abstract), *Lunar Planet. Sci., XX*, 660-661, 1989.

Mellon, M. T., B. M. Jakosky, H. H. Kieffer, and P. R. Christensen, High-resolution thermal inertia mapping from the Mars Global Surveyor Thermal Emission Spectrometer, *Icarus, 148*, 437-455, 2000.

Mustard, J. F., Are dark red soils and bright dust on Mars related through mineralogic phase changes? (abstract), *Lunar Planet. Sci., XXVI*, 1021-1022, 1997.

NASA and Hubble Heritage Team, Hubble captures best view of Mars ever obtained from Earth, http://heritage.stsci.edu/public/2001jul/display.html, Space Telescope Science Institute public release, July 5, 2001.

Peterfreund, A. R., Visual and infrared observations of wind streaks on Mars, *Icarus, 45*, 447-467, 1981.

Pollack, J. B., M. E. Ockert-Bell, and M. K. Shepard, Viking lander image analysis of Martian atmospheric dust, *J. Geophys. Res., 100*, 5235-5250, 1995.

Presley, M. A., The origin and history of surficial deposits in the central equatorial region of Mars, M. S. Thesis, 77 p., Washington University, St. Louis, Missouri, 1986.

Presley, M. A., and R. E. Arvidson, Nature and origin of materials exposed in the Oxia Palus–Western Arabia–Sinus Meridiani region, Mars, *Icarus, 75*, 499-517, 1988.

Pye, K., The nature, origin and accumulation of loess, *Quaternary Science Reviews, 14*, 653-667, 1995.

Sagan, C., J. Veverka, P. Fox, R. Dubisch, J. Lederberg, E. Levinthall, L. Quam, R. Tucker, J. B. Pollack, and B. A. Smith, Variable features on Mars: Preliminary Mariner 9 television results, *Icarus, 17*, 346-372, 1972.

Sagan, C., J. Veverka, P. Fox, R. Dubisch, R. French, P. Gierasch, L. Quam, J. Lederberg, E. Levinthal, R. Tucker, B. Eross and J. B. Pollack, Variable features on Mars, 2, Mariner 9 global results, *J. Geophys. Res., 78*, 4163-4196, 1973.

Sagan, C., D. Pieri, P. Fox, R. E. Arvidson, and E. A. Guinness, Particle motion on Mars inferred from the Viking lander cameras, *J. Geophys. Res., 82*, 4430-4438, 1977.

Schaber, G. G., Radar, visual, and thermal characteristics of Mars: Rough planar surfaces, *Icarus, 42*, 159-184, 1980.

Scott, D. H., and K. L. Tanaka, Geologic map of the western equatorial region of Mars, scale 1:15,000,000, *U.S. Geol. Surv. Misc. Inv. Ser. Map I-1802-A*, 1986.

Sharp, R. P., Wind ripples, *J. Geology, 71*, 617-636, 1963.

Singer, R. B., E. Cloutis, T. L. Roush, P. J. Mouginis-Mark, B. R. Hawke, and P. R. Christensen, Multispectral analysis of the Kasei Vallis-Lunae Planum region, Mars (abstract), *Lunar Planet. Sci., XV*, 794-795, 1984.

Soderblom, L. A., K. Edwards, E. M. Eliason, E. M. Sanchez, and M. P. Charette, Global color variations on the Martian surface, *Icarus, 34*, 446-464, 1978.

Strickland, E. L., Physical properties of Oxia/Lunae Planum and Arabia-type units in the central equatorial region of Mars (abstract), *Lunar Planet. Sci., XX*, 1079-1080, 1989.

Thomas, P., Martian intracrater splotches: Occurrence, morphology, and colors, *Icarus, 57*, 205-227, 1984.

Thomas, P., and P. J. Gierasch, Dust devils on Mars, *Science, 230*, 175-177, 1985.

Thomas, P., and J. Veverka, Seasonal and secular variation of wind streaks on Mars: An analysis of Mariner 9 and Viking data, *J. Geophys. Res., 84*, 8131-8146, 1979.

Thomas, P., and J. Veverka, Red/violet contrast reversal on Mars: Significance for eolian sediments, *Icarus, 66*, 39-55, 1986.

Thomas, P., J. Veverka, S. Lee and A. Bloom, Classification of wind streaks on Mars, *Icarus, 45*, 124-153, 1981.

Tomasko, M. G., L. R. Doose, M. Lemmon, P. H. Smith, and E. Wegryn, Properties of dust in the Martian atmosphere from the imager on Mars Pathfinder, *J. Geophys. Res., 104*, 8987-9007, 1999.

Tsoar, H., and K. Pye, Dust transport and the question of desert loess formation, *Sedimentology, 34*, 139-153, 1987.

Veverka, J., P. Thomas and R. Greeley, A study of variable features on Mars during the Viking Primary Mission, *J. Geophys. Res., 82*, 4167-4187, 1977.

Ward, A. W., K. B. Doyle, P. J. Helm, M .K. Weisman, and N. E. Witbeck, Global map of eolian features on Mars, *J. Geophys. Res., 90*, 2038-2056, 1985.

Wasson, R. J., and R. Hyde, Factors determining desert dune type, *Nature, 304*, 337-339, 1983.

Wentworth, C. K., A scale of grade and class terms for clastic sediments, *J. Geology, 30*, 377-392, 1922.

Wyatt, M. B., J. L. Bandfield, H. Y. McSween, Jr., and P. R. Christensen, Compositions of low albedo intracrater materials and wind streaks on Mars: Examination of MGS TES data in western Arabia Terra, *Lunar Planet. Sci.* [CD-ROM], *XXXII*, abstract 1872, 2001.

Zimbelman, J. R., Surface properties of the Pettit wind streak on Mars: Implications for sediment transport, *Icarus, 66*, 83-93, 1986.

Zimbelman, J. R., and R. Greeley, Surface properties of ancient cratered terrain in the northern hemisphere of Mars, *J. Geophys. Res., 87*, 10181-10189, 1982.

Zimbelman, J. R., and H. H. Kieffer, Thermal mapping of the northern equatorial and temperate latitudes of Mars, *J. Geophys. Res., 84*, 8239-8251, 1979.

Zimbelman, J. R., and S. H. Williams, Wind streaks: Geological and botanical effects on surface albedo contrast, *Geomorphology, 17*, 167-185, 1996.

Zimbelman, J. R., S. H. Williams, and V. P. Tchakerian, Sand transport paths in the Mojave Desert, southwestern United States, in *Desert Aeolian Processes*, edited by V. P. Tchakerian, pp. 101-129, Chapman and Hall, London, 1995.

K. S. Edgett, Malin Space Science Systems, Inc., P.O. Box 910148, San Diego, CA 92191-0148, USA. (Please do not publish e-mail address: edgett@msss.com).

Figure Captions

Figure 1. Western Arabia Terra; 153 craters include wind streaks (usually dark) that emanate from the south ends of craters and extend tens to over a hundred kilometers toward the south. The Viking "color units" of *Arvidson et al.* [1989] and *Presley and Arvidson* [1988] are indicated. Note that most dark wind streaks have a narrow bright red margin. Map is a mosaic of Viking orbiter images from the U. S. Geological Survey.

Figure 2. Dust plume emanating from the Great Sand Dunes National Monument, Colorado, on April 18, 2000 (22:49 UTC). Blowing sand impinging upon crusted soils, playas, and other dust sources can lead to suspension and extension of plumes for hundreds of kilometers downwind. NOAA-14 Advanced Very High Resolution Radiometer image; the difference between bands 4 (10.3–11.3 μm) and 5 (11.5–12.5 μm) allows silicate particles in the dust plume to appear bright relative to H_2O clouds and land/lake surfaces. Image courtesy of NOAA, U.S. National Oceanic and Atmospheric Administration.

Figure 3. Range of low albedo surface types on Mars. (a) Sand dunes, north polar region, M00-01460, 76.6°N, 258.8°W. (b) Sand sheet, Gangis Chasma, M03-02943, 7.7°S, 49.5°W. (c) Smooth-surfaced mantle, Sinus Sabaeus, E02-00623, 6.9°S, 344.5°W. (d) Dark mesa-forming unit, west Candor Chasma, M18-01893, 6.3°S, 74.8°W. (e) Volcanic bedrock among sand dunes

in Meroe Patera, E04-01239, 7.1°N, 291.9°W. In each, illumination is from the left and north is toward the top/upper right.

Figure 4. Typical western Arabia dark streak. (a) Context view of crater at 10.9°N, 347.8°W (top, center) with locations of MOC narrow angle images M07-06117, M19-01943, and E02-02843 indicated. Solid white rectangles indicate locations of sub-frames used in Figures 4b–h. This is MOC WA image M07-06118. (b) Dunes on crater floor in M07-06117; "relative albedo" is between Figures 4b–e is preserved in lower portion of each. (c) Lower south crater wall in M07-06117. (d) Dark mantled streak surface in M07-06117. (e) Southern end of dark streak surface in M07-06117. (f) Dark streak, bright margin, and adjacent terrain in E02-02843 (refer to Figure 4a for context). (g, h) Comparison of intracrater dunes in September 1999 (M07-06117) and September 2000 (M19-01943); no changes are observed. (i) Dunes trapped in small crater (top) on floor of the larger crater at 10.9°N, 347.8°W. Dark material covers the surface in a wedge-shaped region projecting southward from the intracrater dunes; this dark material obscures or reduced contrast between small light-toned bedforms (as seen to the right of the streak) and surrounding terrain. All pictures illuminated from the left.

Figure 5. Dark material deflated from dune trapped in small depression on floor of west Arabia Terra crater at 16.6°N, 15.3°W. This dune and associated sand drifts and wind streak is similar to

the configuration in Figure 4i, and may be a miniature analog for the large dark streaks of western Arabia. E05-00437, illuminated from the left.

Figure 6. Curie Crater dark spot, 29.1°N, 4.8°W. (a) Context view, from M01-01240, showing Curie Crater, its dark spot, its lack of a dark streak that emanates from the spot, and location of the two MOC NA images of the dark spot. No dunes are present in either NA image. Patchy clouds obscure portions of the south and west parts of the context view. (b) Detailed view of dark spot surface in E04-01360. Both pictures illuminated from the lower left.

Figure 7. Dark mesa-forming unit in western Crommelin Crater. (a) Context showing Crommelin Crater, located at 5.1°N, 10.3°W, WA image M20-00871. (b) High resolution view, showing smooth-surfaced dark mesa-forming unit overlying light-toned, rugged surface of layered outcrops materials, image M20-00870. Both pictures illuminated from the left/upper left.

Figure 8. Crater interiors in western Arabia Terra that exhibit light-toned layering (o) and dark mesa-forming units (x). For reference, craters in which at least one MOC NA image was obtained through June 2001 are indicated by small square dots. Map of Viking orbiter image mosaics from the U. S. Geological Survey.

Figure 9. Dark mesa-forming units along intercrater boundary between northern Terra Meridiani and western Arabia Terra. Dark mesa-forming material overlies a previously-eroded surface, FHA-00674, near 1.7°N, 357.1°W, illuminated from the left/upper left.

Figure 10. Light-toned layer outcrop mounds (arrows) in (a) Trouvelot Crater (16.3°N, 13.0°W; mosaic of M01-00459, M01-01444, M01-01446) and (b) Becquerel Crater (22.3°N, 8.3°W; M01-00849); north is up, illumination from the left.

Figure 11. Detail of light-toned layer outcrops in crater at 8°N, 7°W. Arrows indicate a fault across which cliff-bench layer exposures are off-set. Dark sand drifts accentuate contrast between layers. E05-00804, illuminated from the left/lower left.

Figure 12. Light-toned layered outcrops in western Arabia Terra craters might serve as a local source for light-toned sediment that in some places forms streaks and light-toned margins around dark streaks. This example from a crater located at 2.2°N, 7.8°W, shows light-toned wind streaks shed directly from adjacent light-toned buttes. M09-06275, illuminated from the lower left.

Figure 13. Erosion has exposed alternating light- and dark-toned layers in the Becquerel Crater layered mound (Figure 10b). Dark layers are inferred to be much thinner and/or less-resistant to

erosion than light-toned layers, because the dark toned layers are not visible from orbit on steeper slopes. The dark-toned layers are about as dark as the eolian megaripples visible at the right and upper right, but are not as dark as sand dunes and drifts seen elsewhere in the full image, M03-03117, from which this sub-frame was cut. Dunes in Becquerel are typically as dark as the darkest feature, a circular depression, in this picture. Centered near 21.6°N, 8.2°W, this scene is illuminated from the lower left.

Figure 14. Typical western Arabia Terra intracrater surfaces outside dune fields and layered units. All examples are from Trouvelot Crater (Figure10a). (a) Rugged and craggy crater floor surface near 17.1°N, 129°W, M02-01093. (b) A second example of typical rugged and craggy crater floor surfaces, near 16.8°N, 13.6°W, M08-07400. (c) Pedestal crater formed by deflation of layer immediately beneath the crater ejecta, which served as a rocky armor to protect the underlying material from removal, near 15.9°N, 13.4°W, E05-01291. (d) Typical wall and rim surfaces are mantled by smooth-surfaced, intermediate-toned material; this example is near 17.5°N, 12.9°W, in M02-01093. All images are illuminated from the left.

Figure 15. The typical western Arabia Terra intercrater plains are mantled by a material that, at the surface, presents the "dark red" color and intermediate albedo described by researchers working with Viking data prior to the MGS mission [e.g., *Arvidson et al.*, 1989]. (a) Example

near Trouvelot Crater at 15.7°N, 11,5°W; CAL-00425. (b) Example near 7.5°N, 354.2°W; M03-02924. Both images are illuminated from the left.

Figure 16. Layered intercrater terrain of western Arabia Terra and dust plumes (arrows) observed on April 1, 1978 by Viking 1. No dust plumes were evident on or near the wind streaks or intracrater dune fields (e.g., upper right corner). The terraced nature of the intercrater plain (especially near image center) indicates layered bedrock exposed by erosion that predates the surficial mantles that presently cover the region (Figure 14). Portion of 653A58, center near 1.9°N, 6.0°W, illuminated from the right.

Figure 17. Example of layered intercrater plains in western Arabia Terra. Buttes in the lower left corner exhibit multiple layers. M03-07310, near 9.8°N, 3.0°W, illuminated from the left/lower left.

Figure 18. Yardangs (ridges running diagonal across the scene) and pedestal craters (circular feature at bottom center) in the intercrater terrain of western Arabia indicate a layered and wind-eroded bedrock. M03-01456, near 14.0°N, 356.1°W, illuminated from the lower left.

Figure 19. Exposures of dark mesa-forming and light-toned layered materials at the southeastern margin of the dark streak emanating from Rutherford Crater near 15.6°N, 10.3°W. (a) Context view of Rutherford Crater and its streak with the location of the high resolution view indicated; M01-00459, illuminated from the left. (b) High-resolution view of dark mesa-forming material (top third of image) and light-toned layered units (lower two-thirds of image) at the margin of Rutherford's dark streak; M07-03968; illuminated from the lower left.

Figure 20. Variety of wind streak changes in western Arabia observed between Viking red filter images from 1978 and MOC red wide angle images from 1999. (a) Some streaks remained largely unchanged, these two have only slightly different configurations between 1978 and 1999; images 829A43 and M01-00847, center near 10.4°N, 6.9°W. (b) Some streaks became brighter relative to their surroundings; images 653A62 and M01-01629, at 5.9°N, 356.2°W. (c) Some streaks largely disappeared; images 653A58 and M01-00847, at 4.2°N, 5.4°W. (d) Some streaks grew longer and/or darker; images 831A18 and M01-00641, at 7.3°N, 353.2°W. Illumination is from the right in the Viking images and from left in the MOC images.

Figure 21. Some dark streaks in western Arabia exhibit evidence of surface and near-surface eolian transport, in this case light-toned wind streaks in the lee of kilometer-scale impact craters

(arrows) are superposed on the larger dark streak surface. Crater at top center is located at 10.8°N, 1.4°W. M01-01238, illuminated from the left.

Figure 22. Most western Arabia Terra dark streaks appear at MOC NA image scales to be thin veneers superposed on a previously mantled surface. (a) MOC WA context image M07-00741 showing location of NA subframe at margin of dark streak near 8.8°N, 346.9°W. (b) NA image of streak margin, there is little difference between the light and dark mantle surfaces except their relative albedo. M07-00740; both images illuminated from the lower left.

Figure 23. Dark filamentary streaks on intracrater dune surfaces in western Arabia Terra are good evidence that dust devils have passed through the region. Multiple streaks are present in each image, a few examples are indicated by arrows. (a) Streaks on low patches of dark sand in E05-00661, near 2.7°N, 9.9°W. (b) Streaks on dune in crater near 8.2°N, 7.3°W, M20-00535. (c) Streaks on relatively light-toned dune in Trouvelot Crater near 16.3°N, 13.4°W, SP2-53203, 16.3°N, 13.0°W. (d) Streaks on rippled dune in crater at 2.4°N, 9.3°W, M19-00188. Each picture is illuminated from left, north is toward the upper right.

Figure 24. Example of test for movement or changes in dune configuration among west Arabia intracrater dune fields. No changes in dune position or shape are observed after a 1.4 Mars years

interval. (a) Dunes in south Trouvelot Crater, 15.4°N, 13.3°W, in September 1998, SP2-53203. (b) The same dunes in June 2001, E05-01291. Both images are illuminated from the left/lower left.

Table 1. Craters with Dunes at Wind Streak Source in Western Arabia Terra From Images Acquired Through June 2001.

Location (latitude, longitude)		Earliest Picture Showing Dunes		
		Spacecraft	Image Number	Year
11.7°N	346.7°W	Mariner 9	DAS 9449589	1972
22.2°N	8.1°W	Viking 1	209A07	1977
17.2°N	4.9°W	Viking 1	212A45	1977
8.9°N	348.9°W	Viking 2	411B14	1977
11.0°N	2.9°W	Viking 1	708A03	1978
1.7°N	351.7°W	Viking 1	709A42	1978
8.0°N	7.0°W	Viking 1	369S34	1980
4.2°N	5.4°W	MGS	AB1-03001	1997
11.0°N	350.9°W	MGS	SP1-26004	1998
22.1°N	22.5°W	MGS	SP2-34903	1998
13.1°N	3.6°W	MGS	SP2-35103	1998
6.7°N	345.8°W	MGS	SP2-40803	1998
21.3°N	17.5°W	MGS	SP2-42304	1998
19.2°N	10.7°W	MGS	SP2-44207	1998
15.5°N	22.2°W	MGS	SP2-51303	1998
16.4°N	13.1°W	MGS	SP2-53203	1998
8.3°N	358.7°W	MGS	M03-02407	1999
5.0°N	10.2°W	MGS	M03-02716	1999
2.3°N	7.8°W	MGS	M03-05599	1999
2.7°N	358.9°W	MGS	M03-06290	1999
13.2°N	18.0°W	MGS	M04-02192	1999
24.6° N	10.8°W	MGS	M04-02970	1999
16.5°N	16.5°W	MGS	M07-00748	1999
2.7°N	9.4°W	MGS	M07-02411	1999
5.7°N	351.5°W	MGS	M07-05541	1999
11.0°N	347.8°W	MGS	M07-06117	1999
10.9°N	1.4°W	MGS	M08-05219	1999
10.1°N	351.9°W	MGS	M11-00086	2000
18.2°N	17.0°W	MGS	M11-00431	2000
13.8°N	23.3°W	MGS	M11-01942	2000
14.9°N	359.0°W	MGS	M20-01694	2000
7.4°N	353.1°W	MGS	M21-00827	2000
10.9°N	4.4°W	MGS	E02-01145	2001
9.2°N	347.7°W	MGS	E02-01236	2001
13.6°N	20.1°W	MGS	E02-02645	2001
12.5°N	0.8°W	MGS	E04-00599	2001
13.8°N	9.8°W	MGS	E04-01032	2001
14.9°N	19.0°W	MGS	E04-01271	2001
16.5°N	15.3°W	MGS	E05-00437	2001
11.0°N	14.0°W	MGS	E05-01993	2001
14.6°N	14.9°W	MGS	E05-01995	2001
13.1°N	7.2°W	MGS	E05-02644	2001
8.5°N	15.8°W	MGS	E05-03231	2001

Table 2. Craters with Known Lack of Dunes at Wind Streak Source in Western Arabia Terra From Images Acquired Through June 2001.

Location (lat., lon.)	Relevant MOC Pictures	Observations and Comments
27.0°N 16.9°W	E04-01503	No wind streak, dark spot has no dunes.
29.0°N 4.7°W	M08-03017 & E04-01360	No wind streak, no dunes; Curie Crater.
17.3°N 354.0°W	M03-04393	No wind streak; small dark patches may be drifts of sand, but no dunes present.
16.0°N 354.7°W	M11-01924 & M23-01170	No wind streak; small dark patches may be drifts of sand, but no dunes present.
2.1°N 349.5°W	M11-01157	Has wind streak; small dark patches may be drifts of sand, coverage may not be complete enough to see larger dunes.

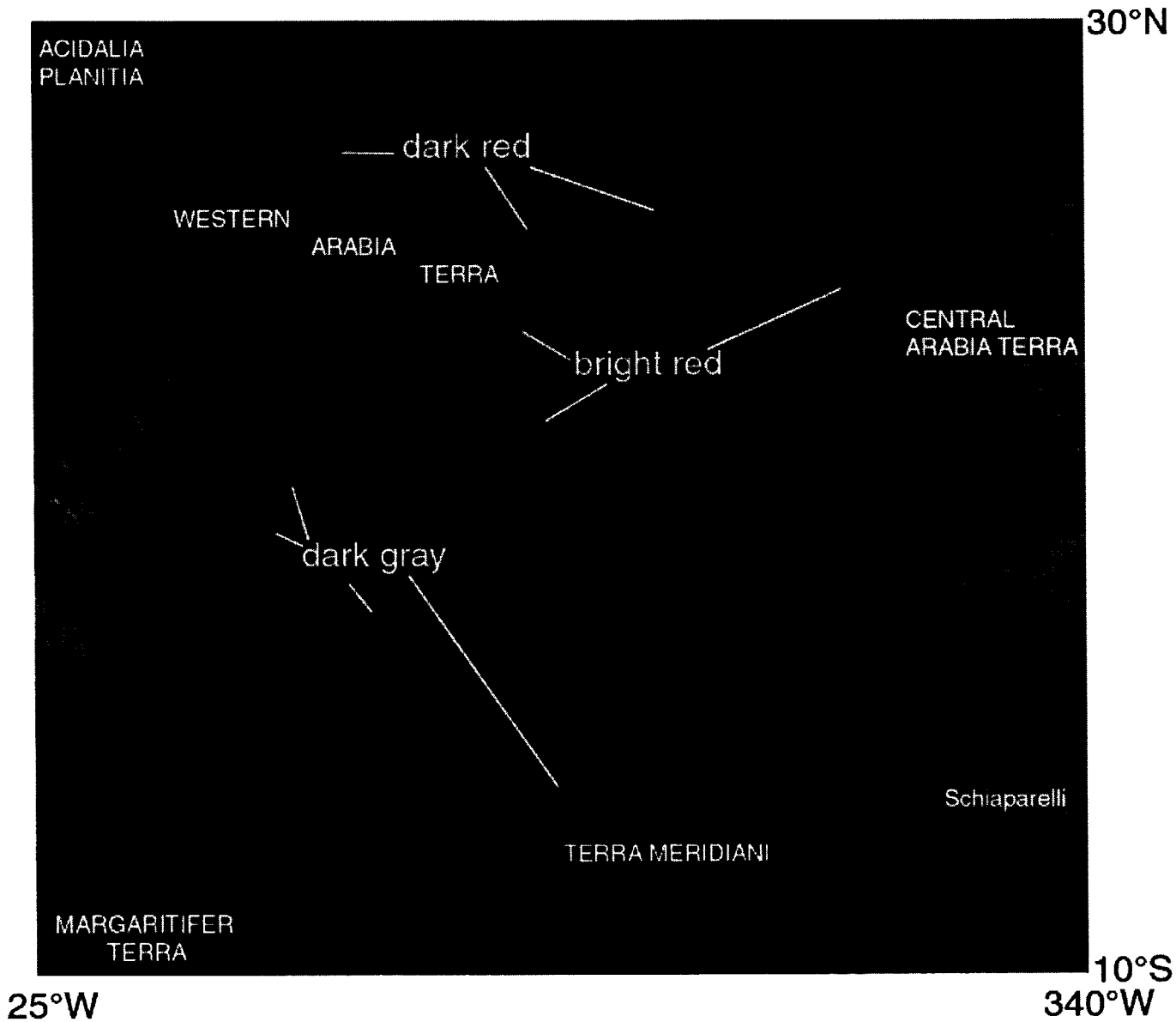
30°N
ACIDALIA
PLANITIA
dark red
WESTERN
ARABIA
TERRA
CENTRAL
ARABIA TERRA
bright red
dark gray
Schiaparelli
TERRA MERIDIANI
MARGARITIFER
TERRA
10°S
25°W
340°W

Figure 1

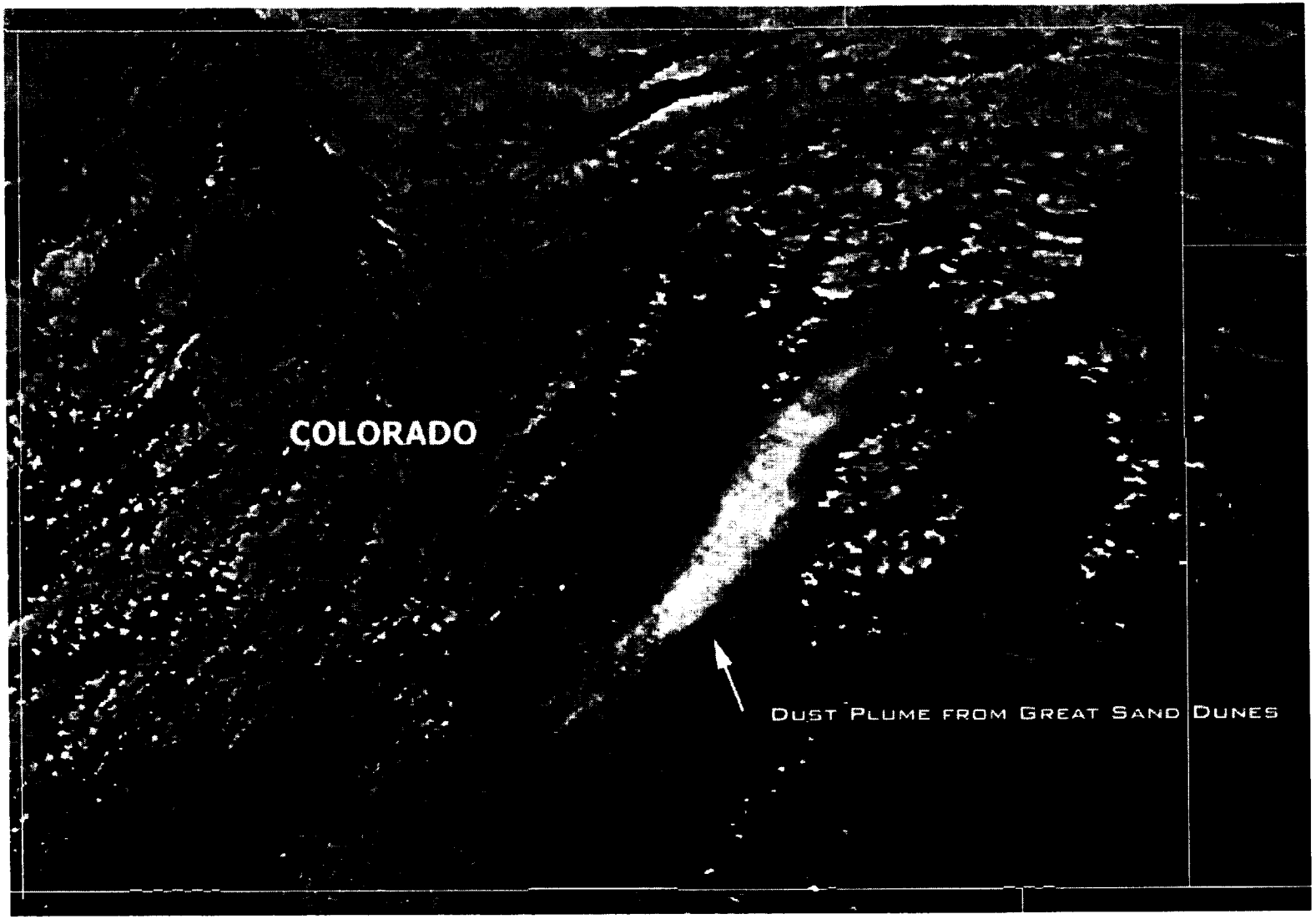

Figure 2

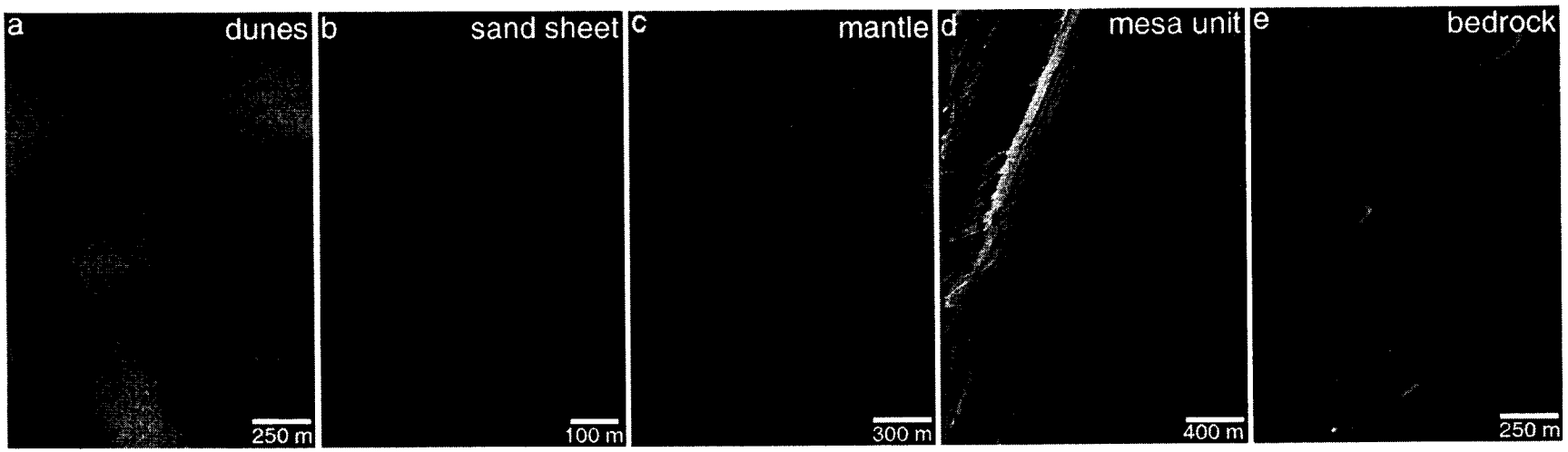
a
dunes
250 m
b
sand sheet
100 m
c
mantle
300 m
d
mesa unit
400 m
e
bedrock
250 m

Figure 3

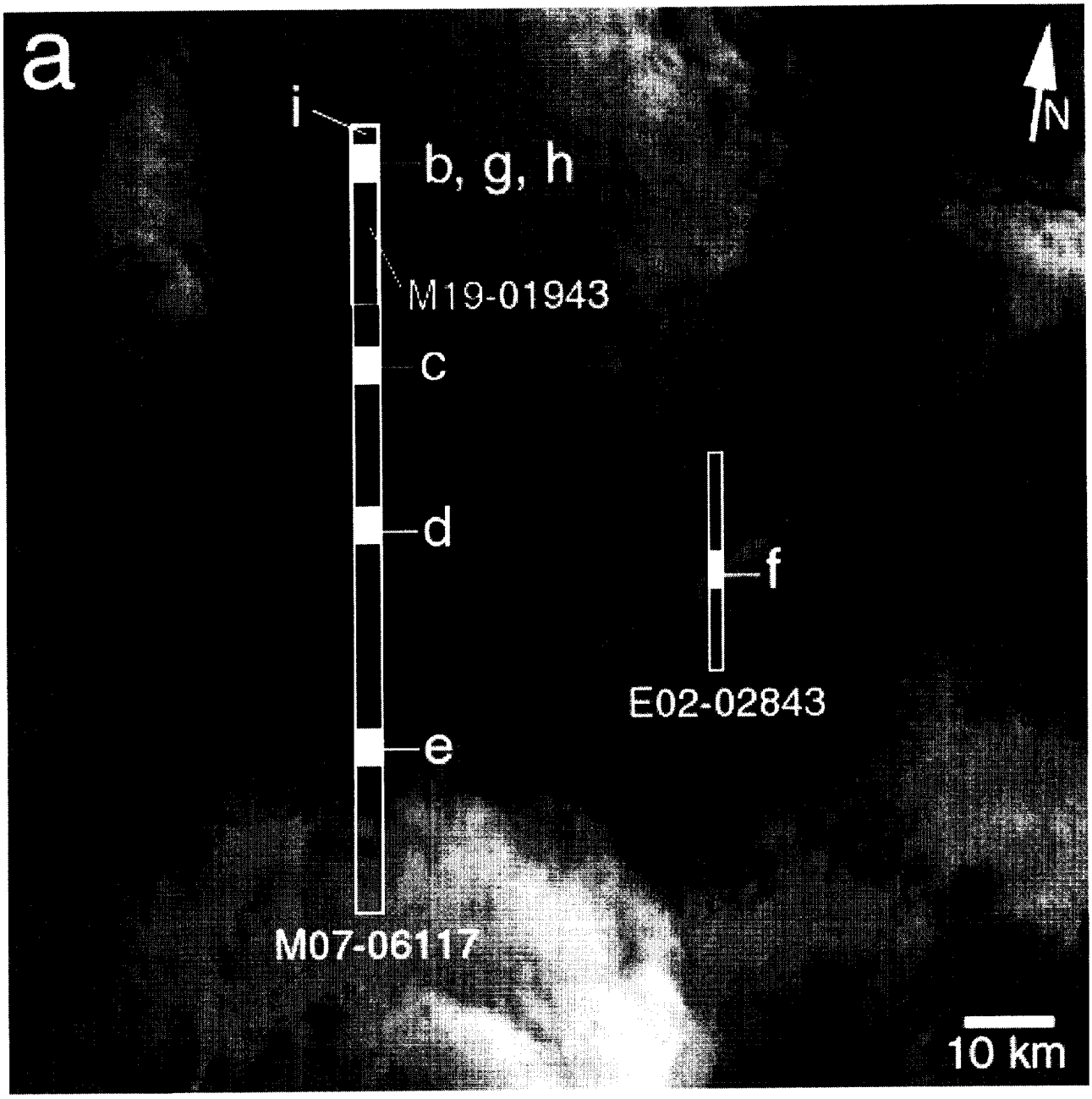

Figure 4a

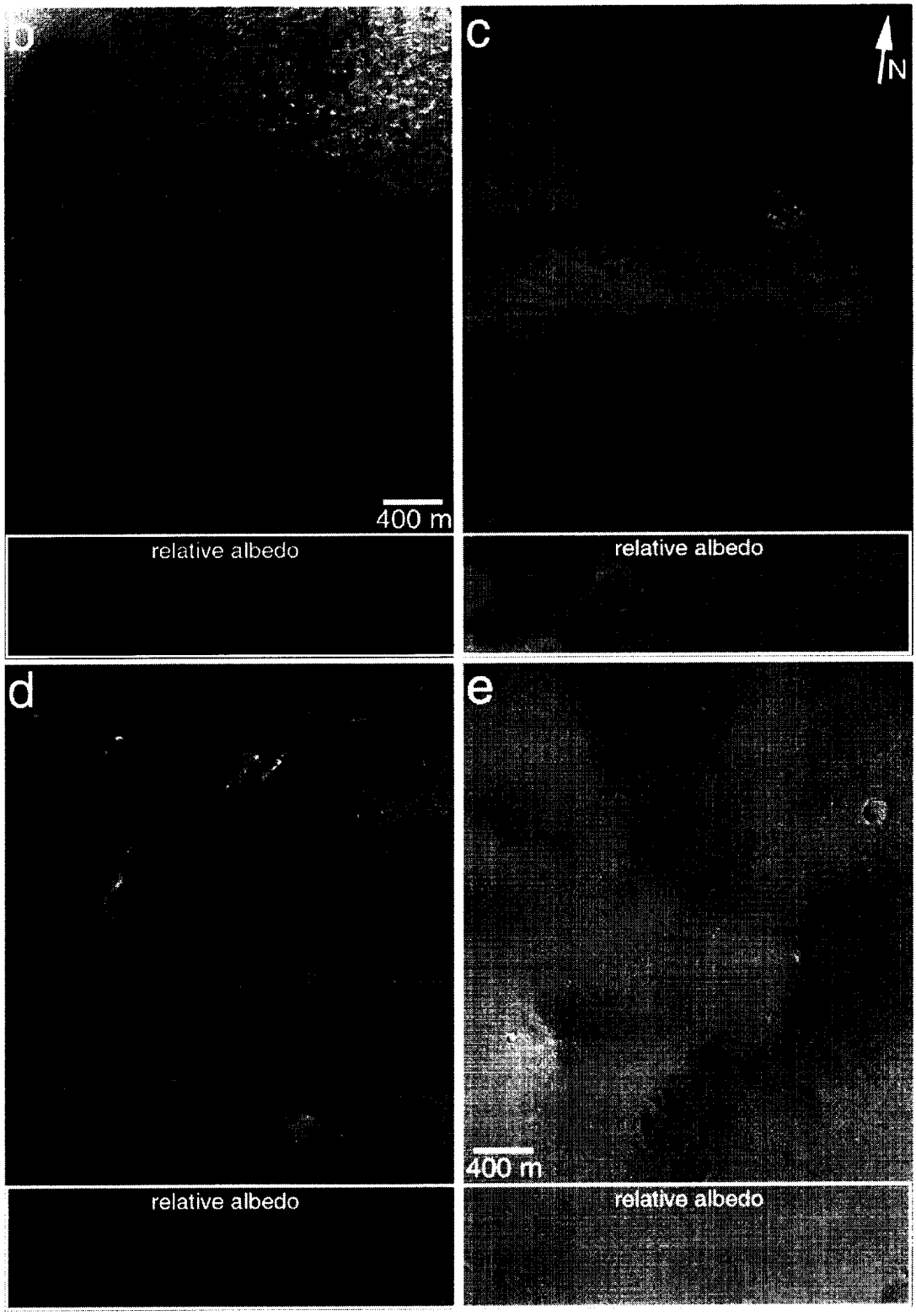
b
400 m
relative albedo
c
N
relative albedo
d
relative albedo
e
400 m
relative albedo

Figure 4b–e

Figure 4f

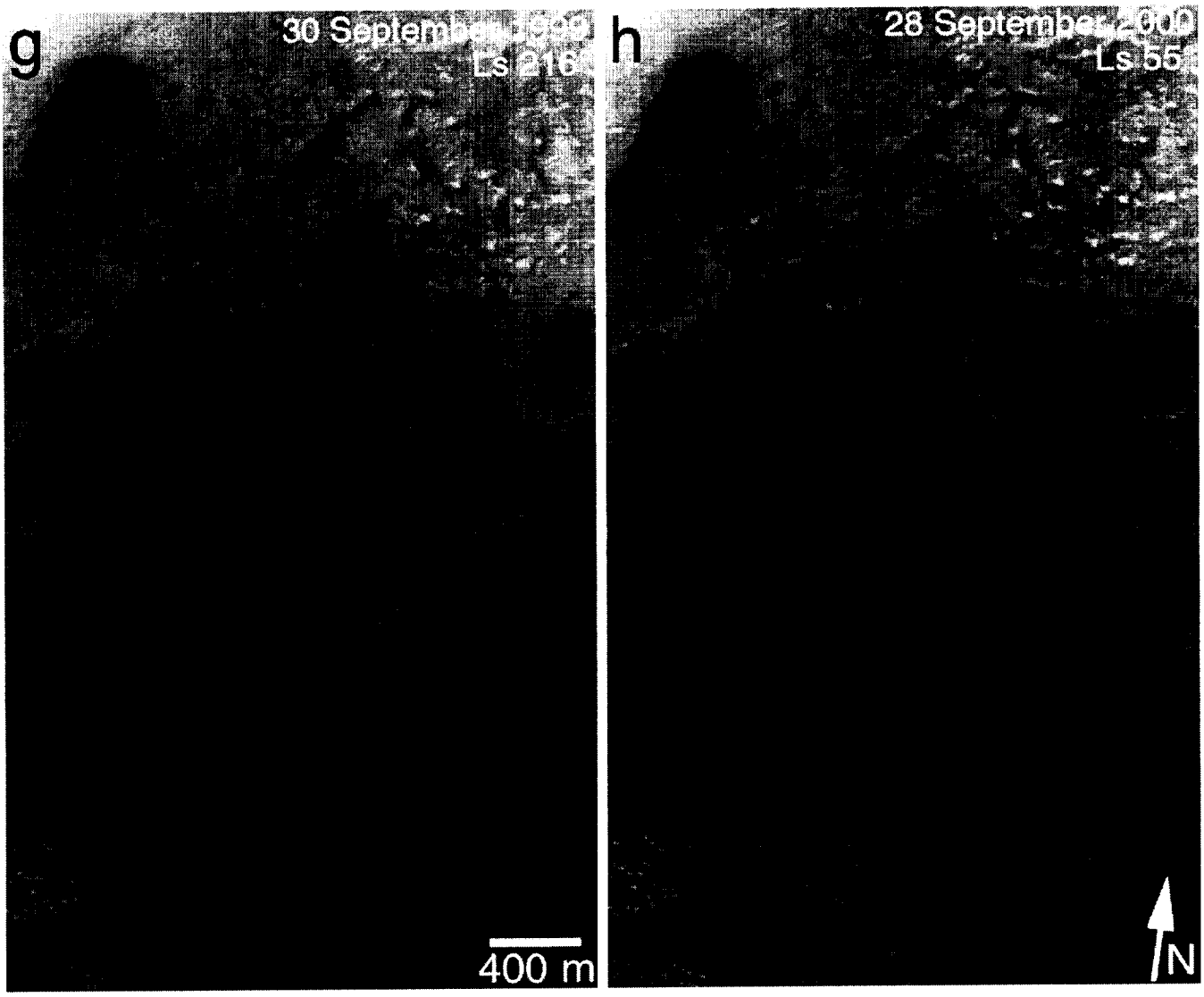

Figure 4g–h

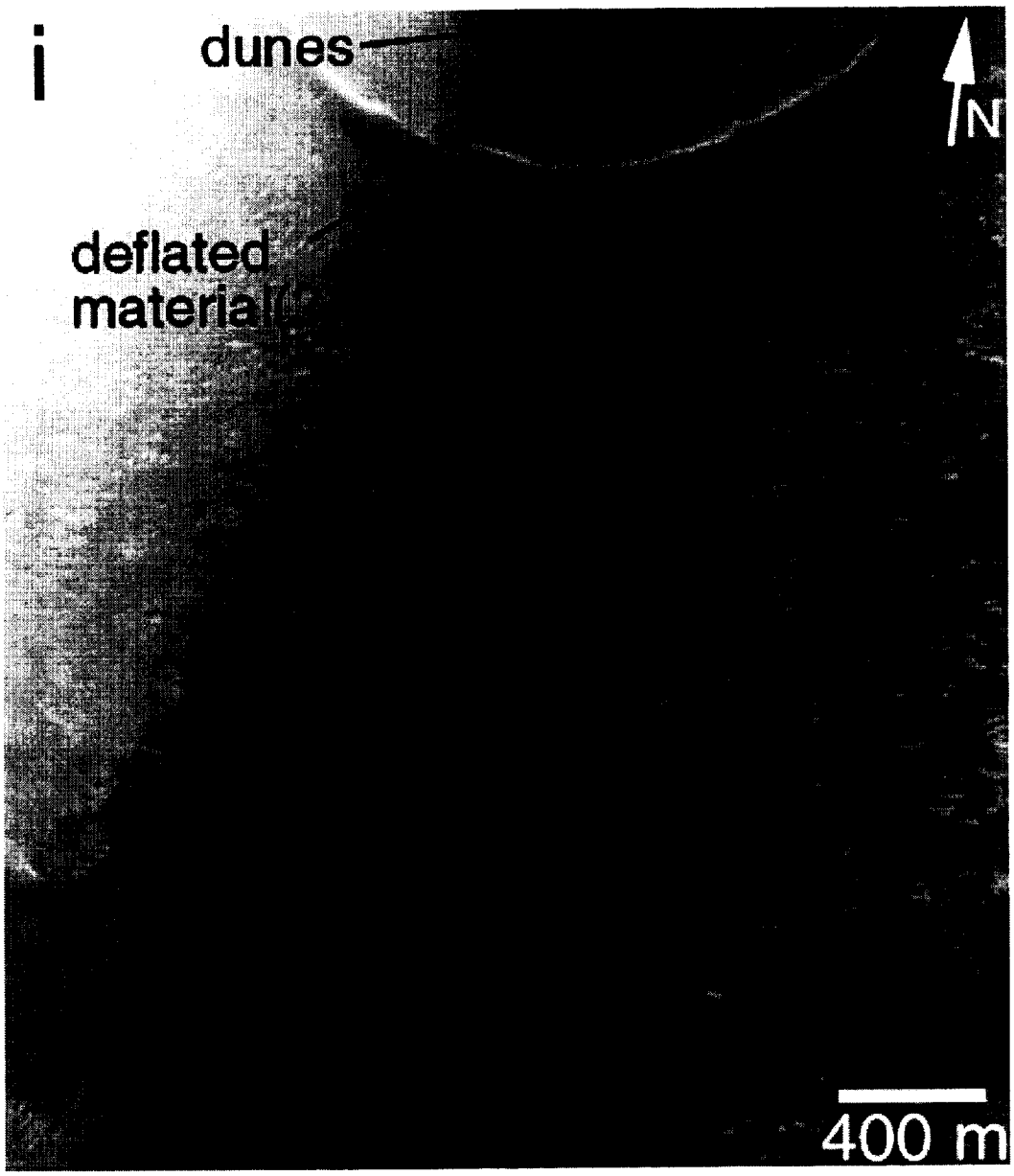

Figure 4i

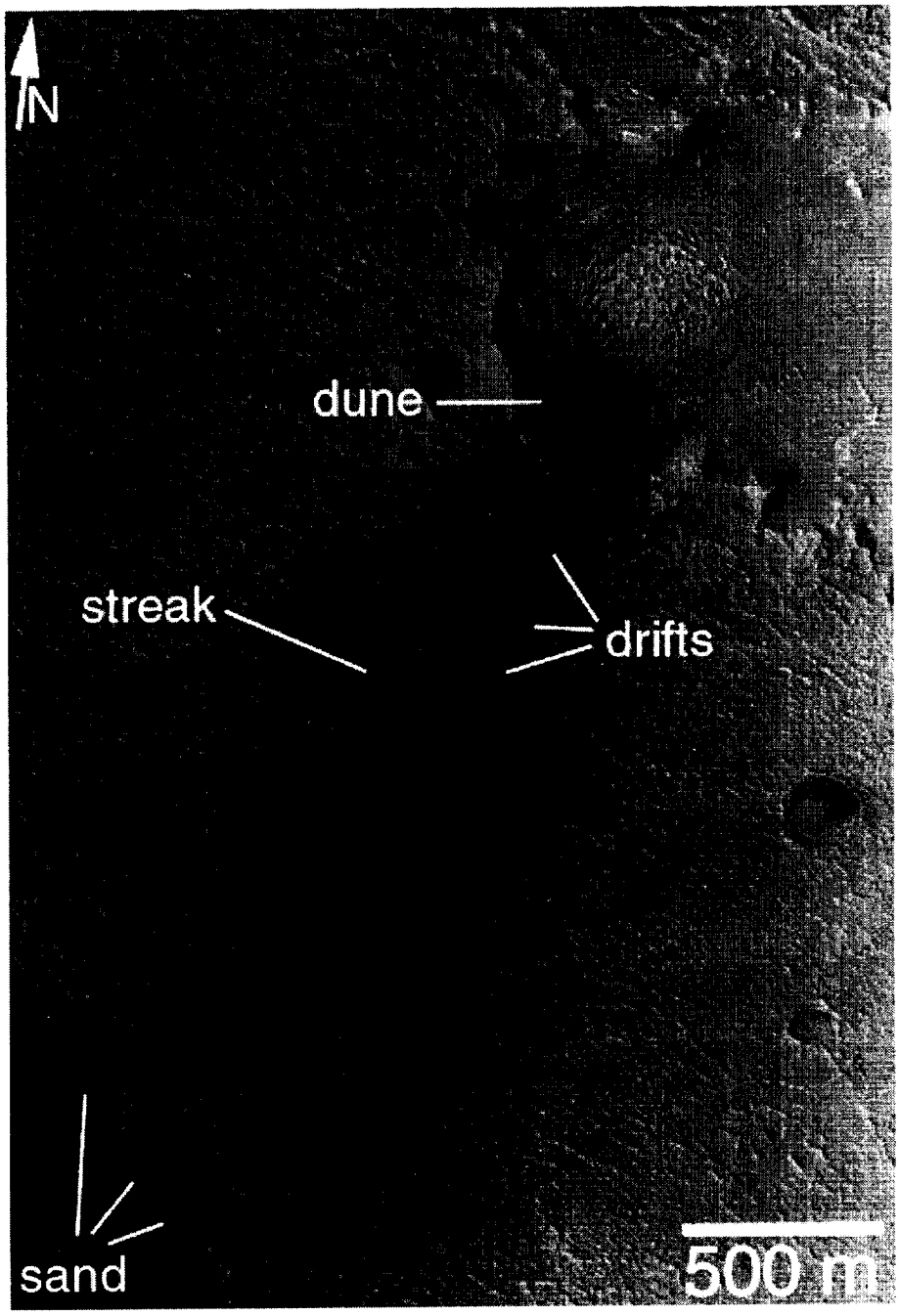

Figure 5

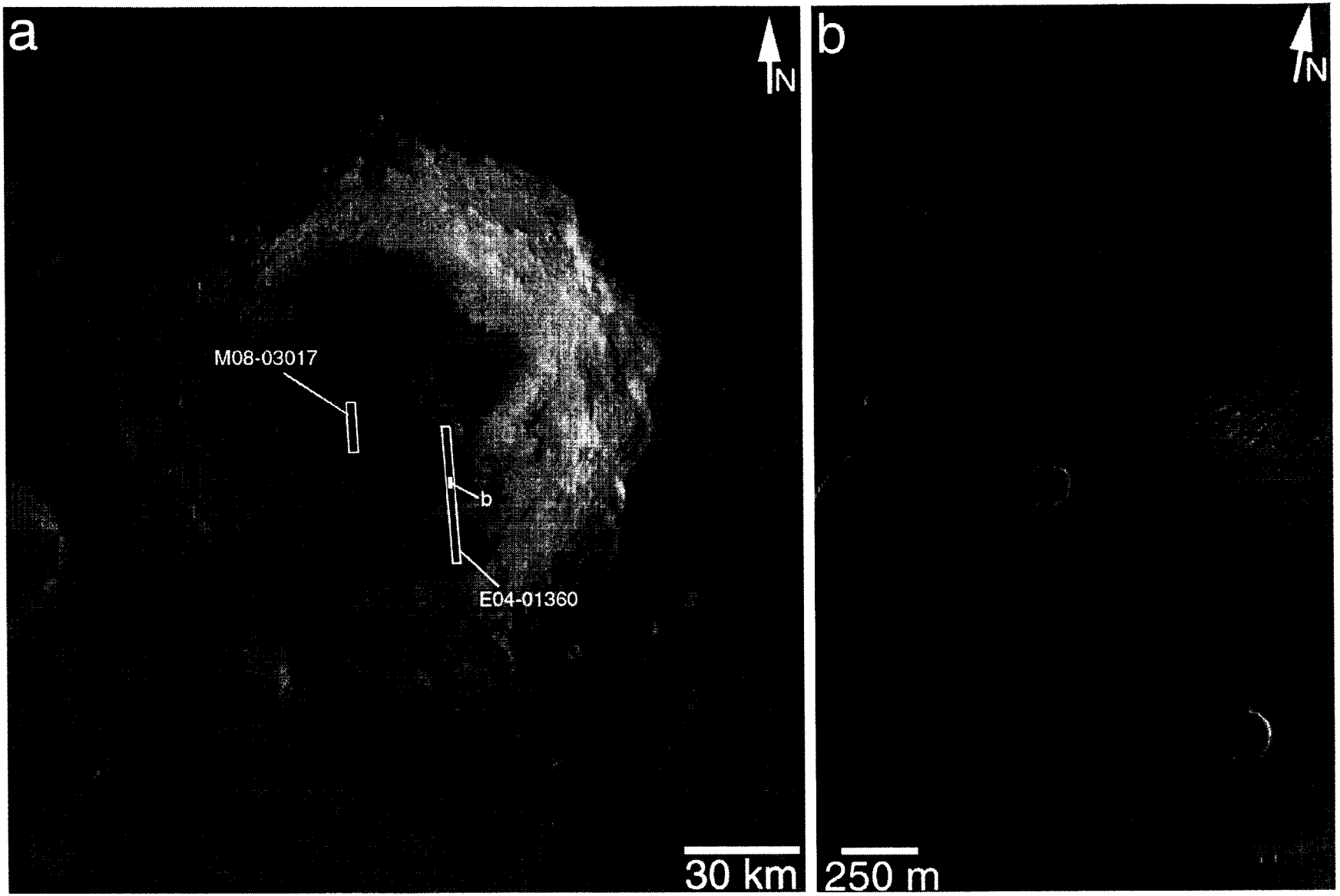

Figure 6

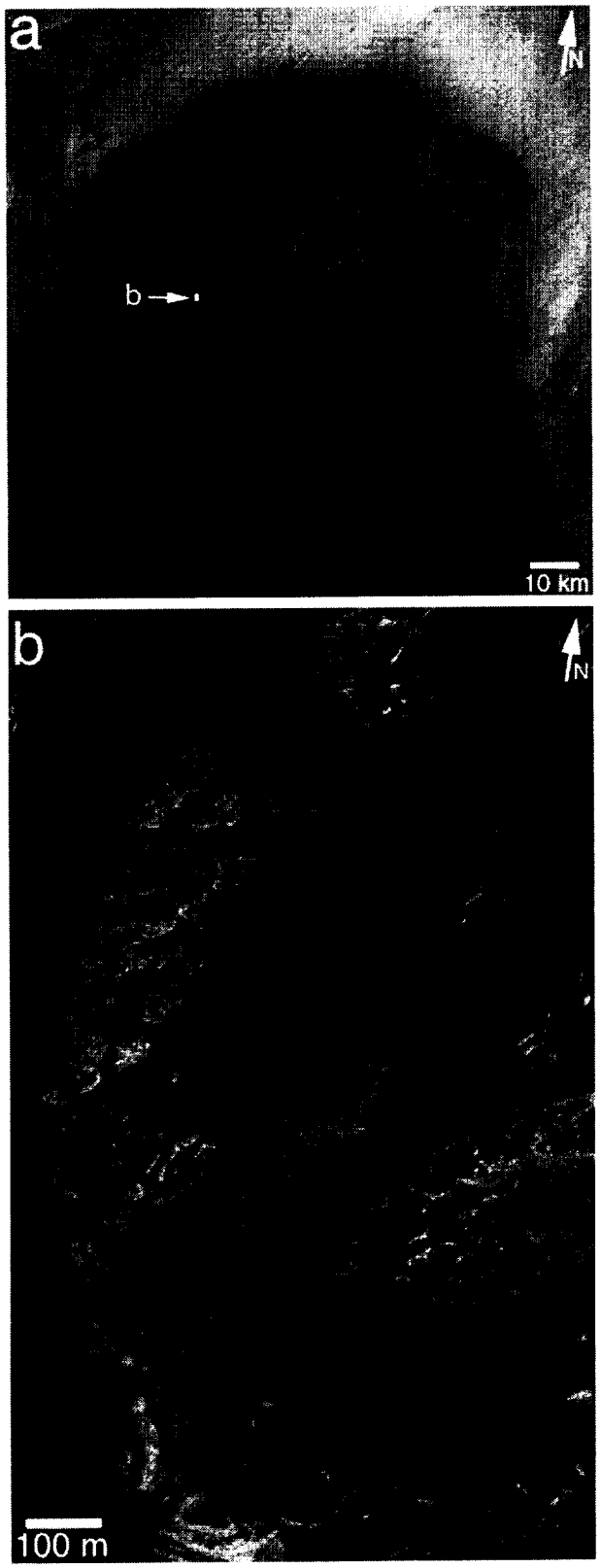

Figure 7


30°N
10°S
25°W
340°W
O layer outcrops
X dark mesa units
craters imaged

Figure 8

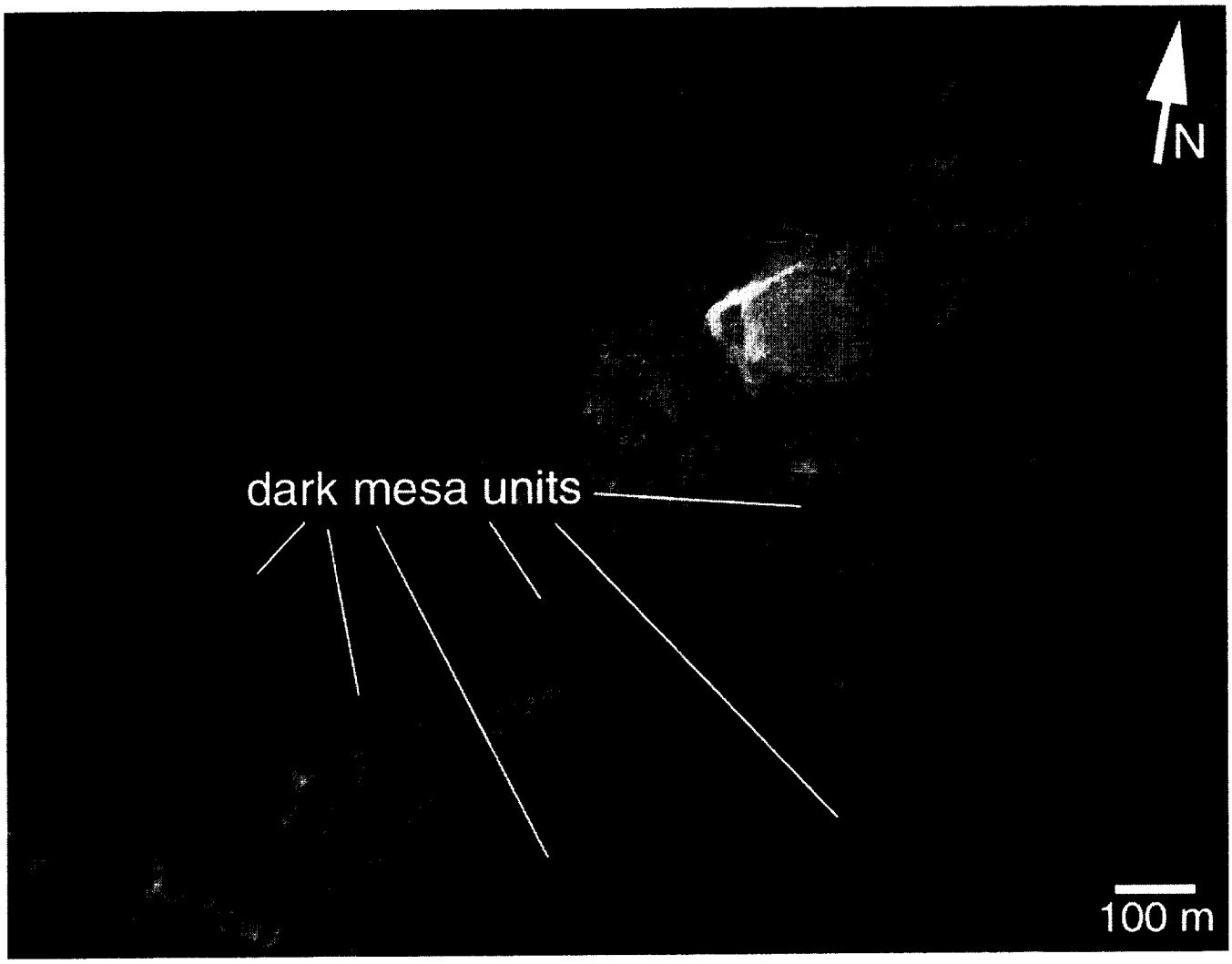

Figure 9

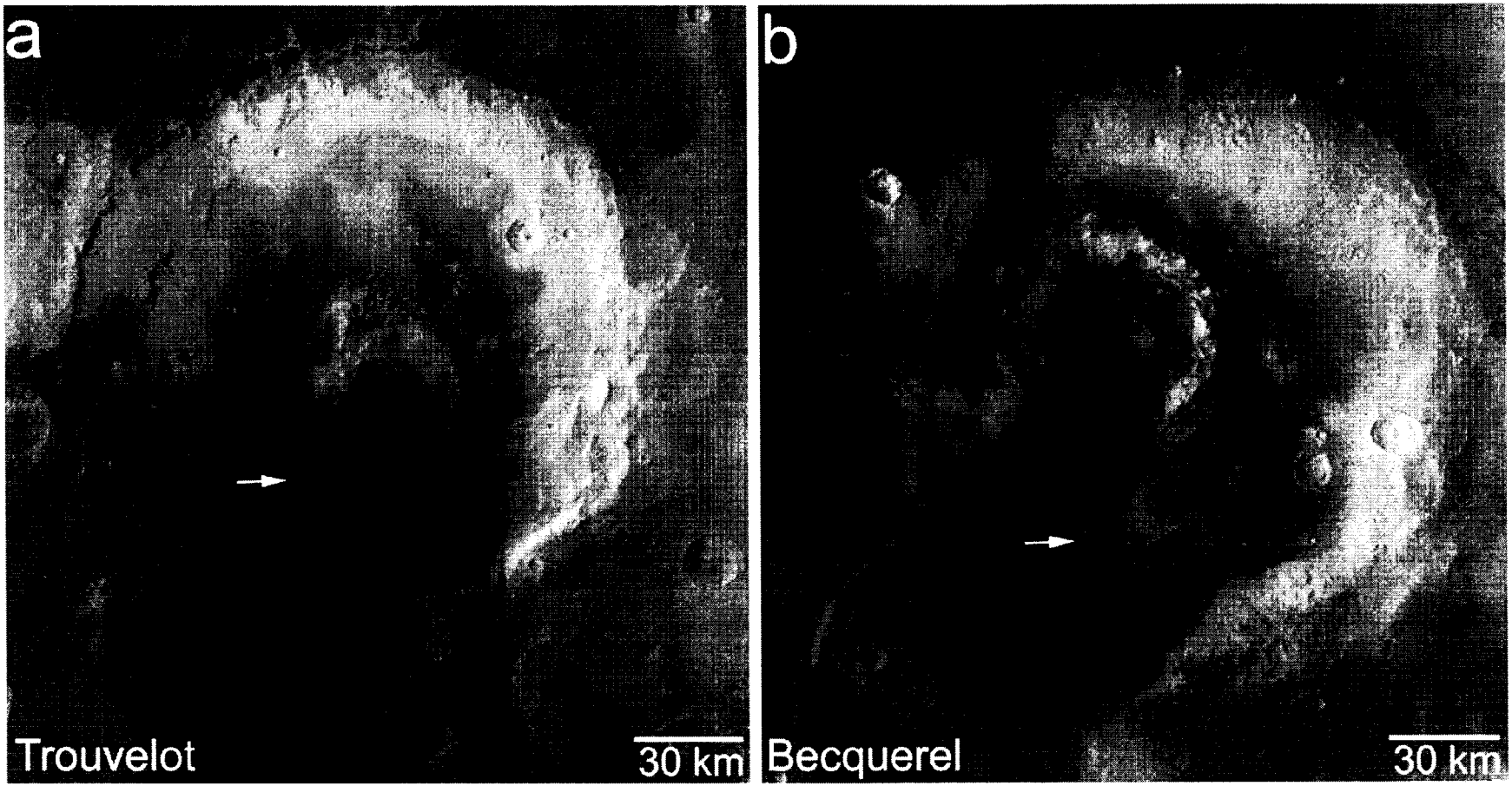

Figure 10

Figure 11

Figure 12

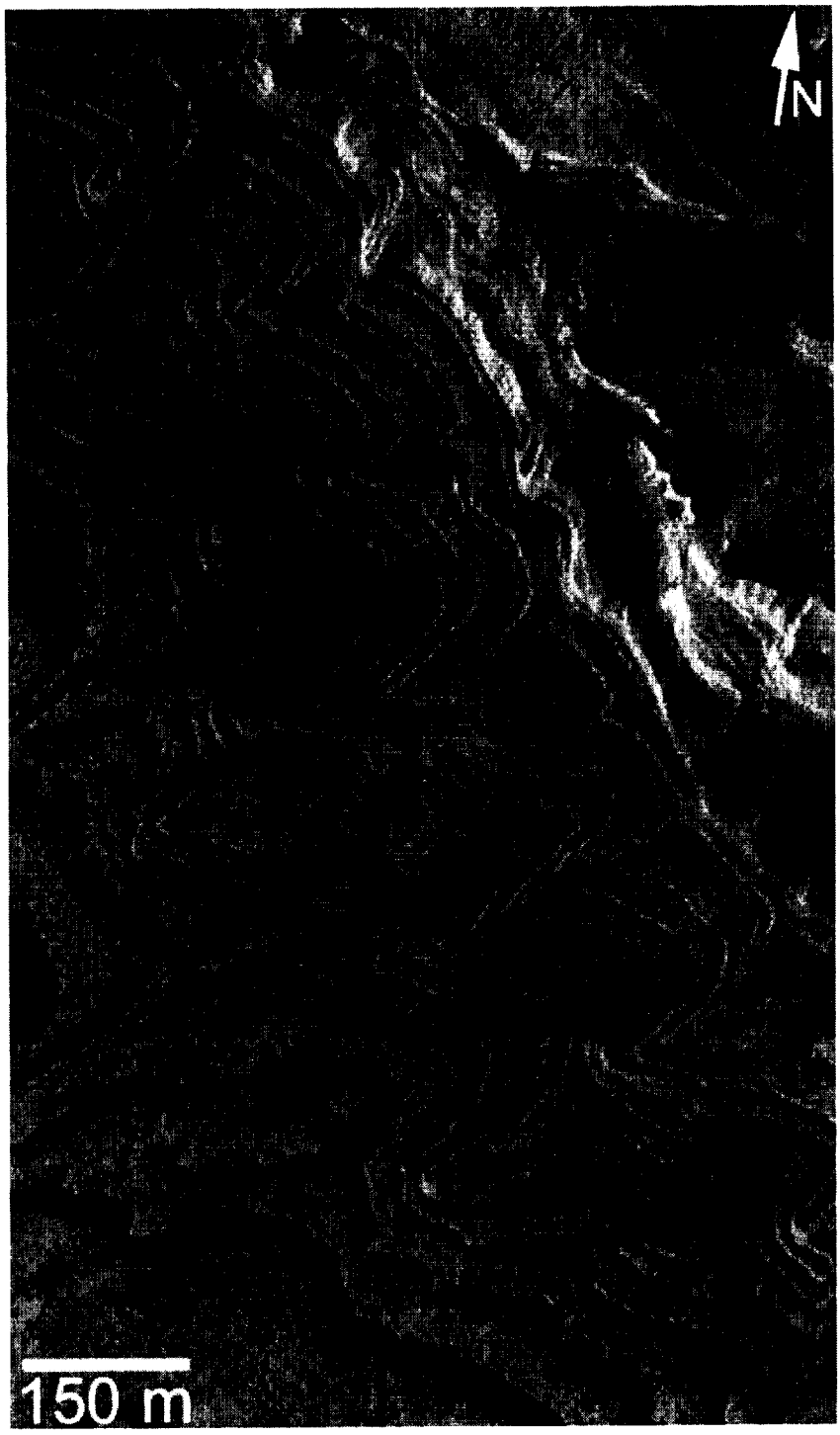

Figure 13

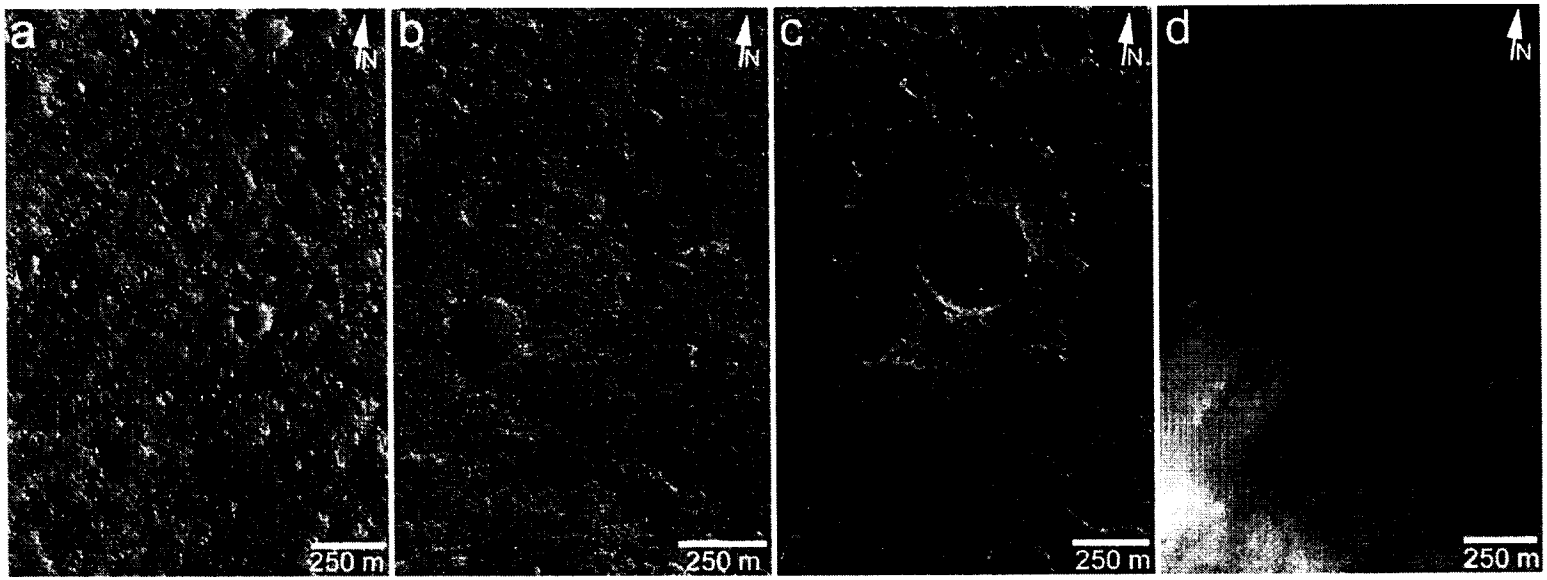

Figure 14

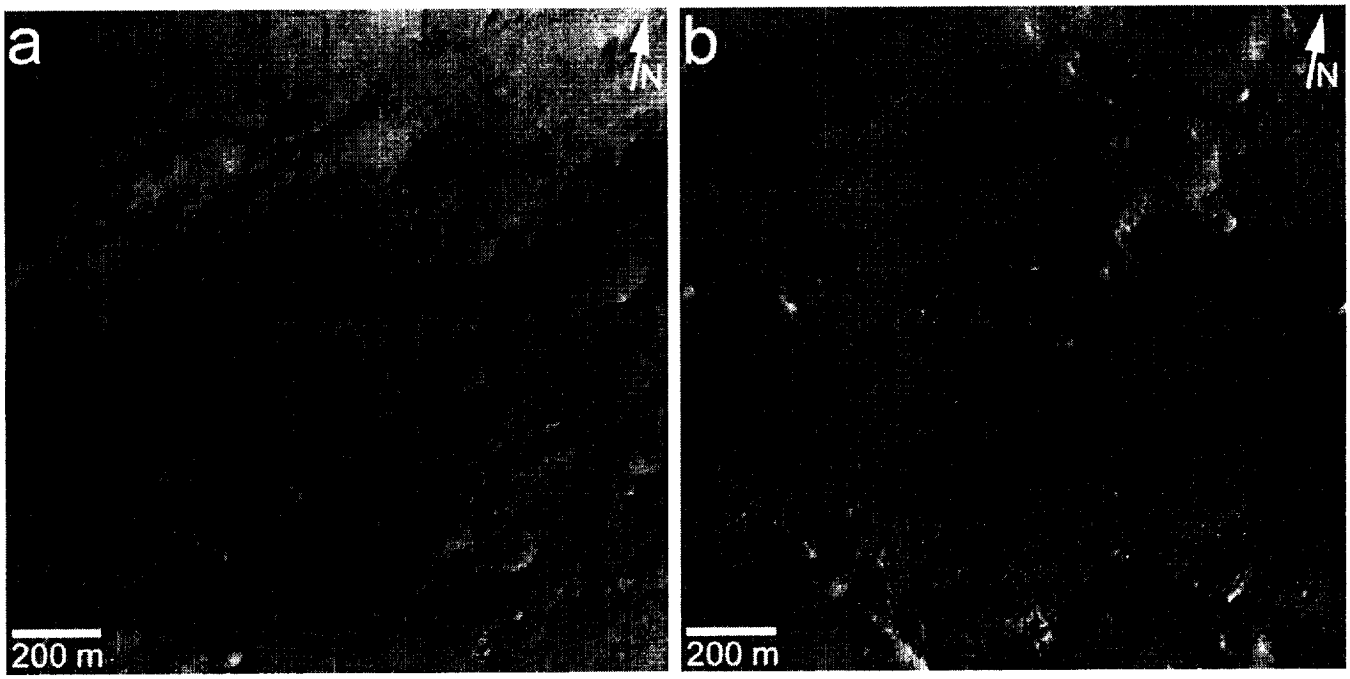

Figure 15

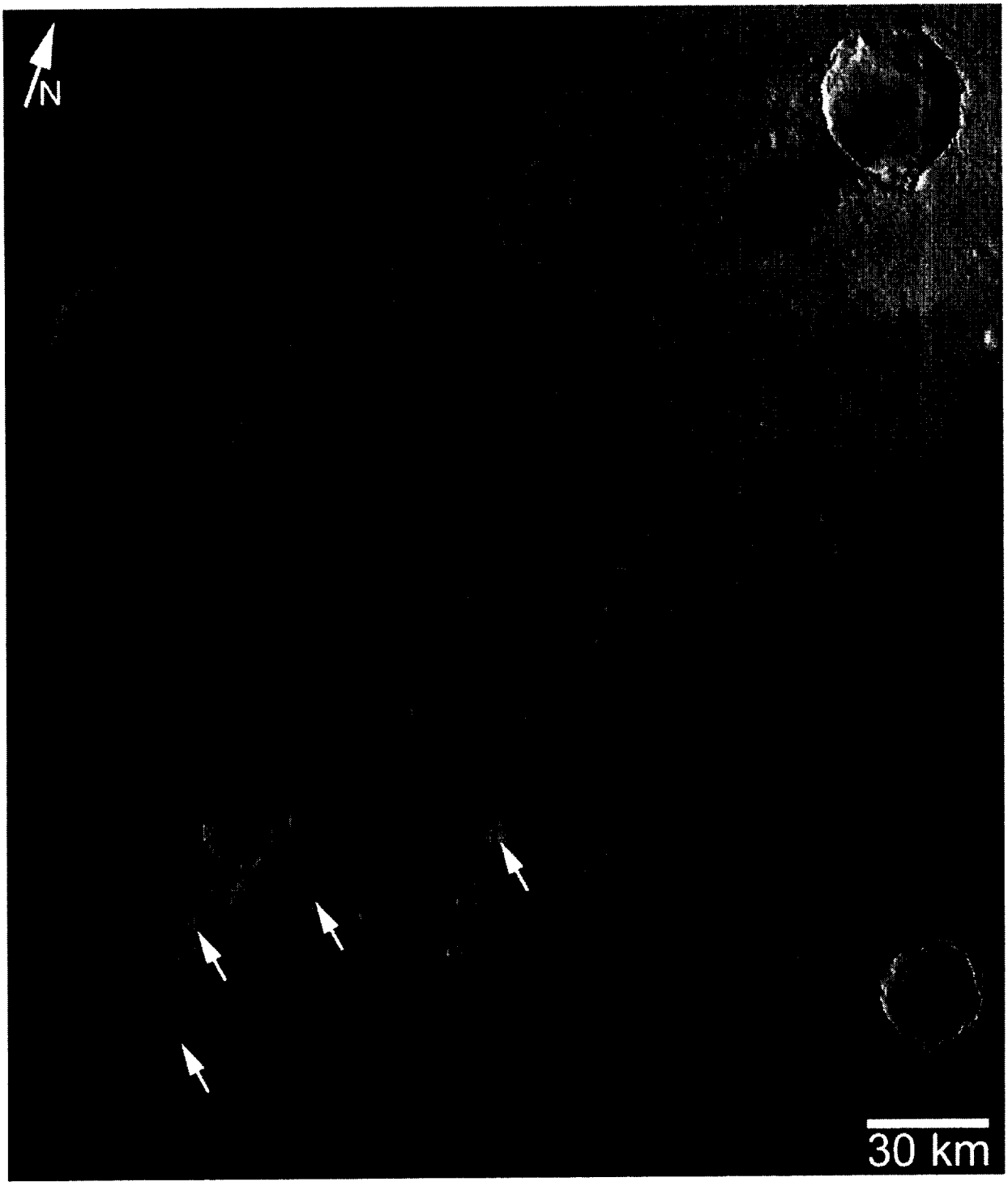

Figure 16

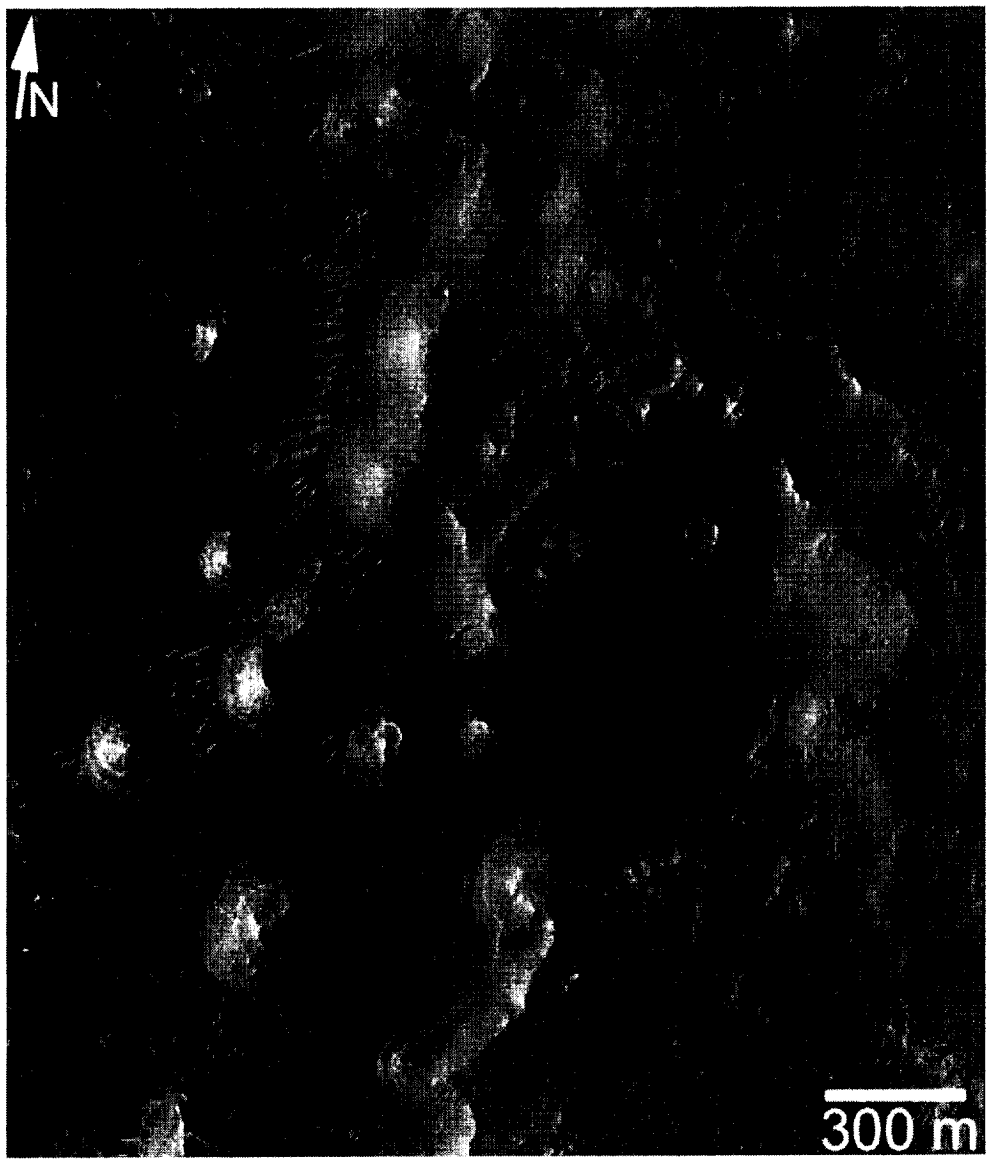

Figure 17

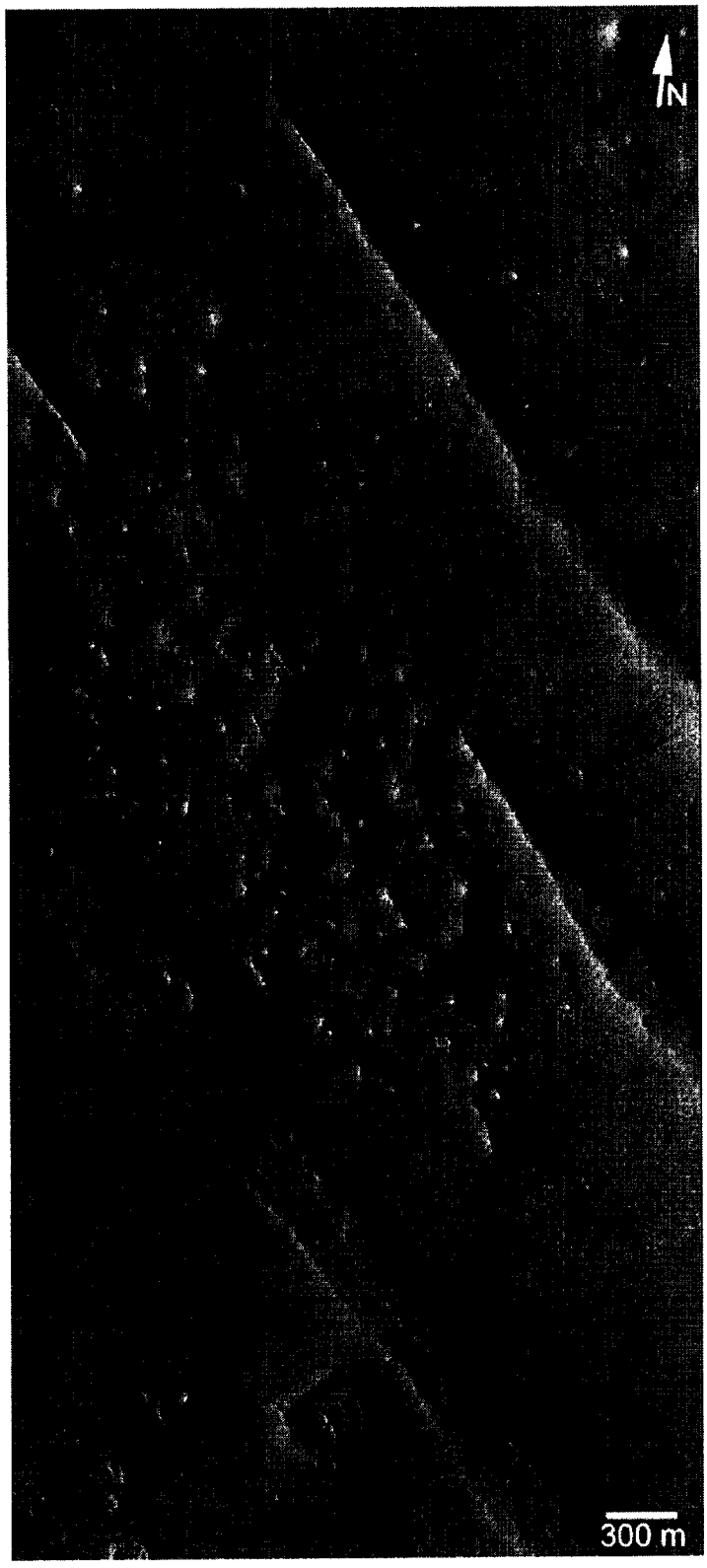

Figure 18

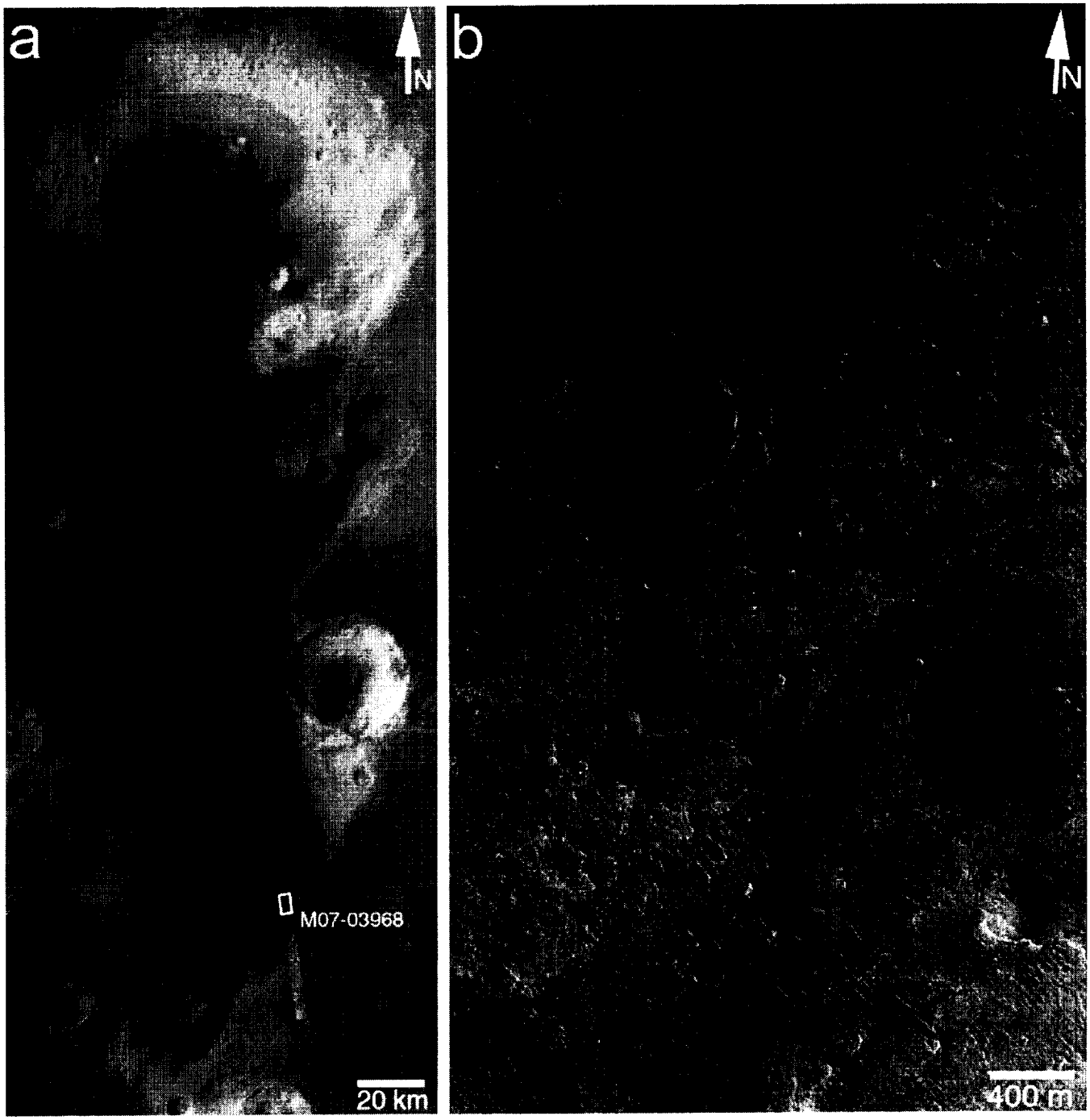

Figure 19

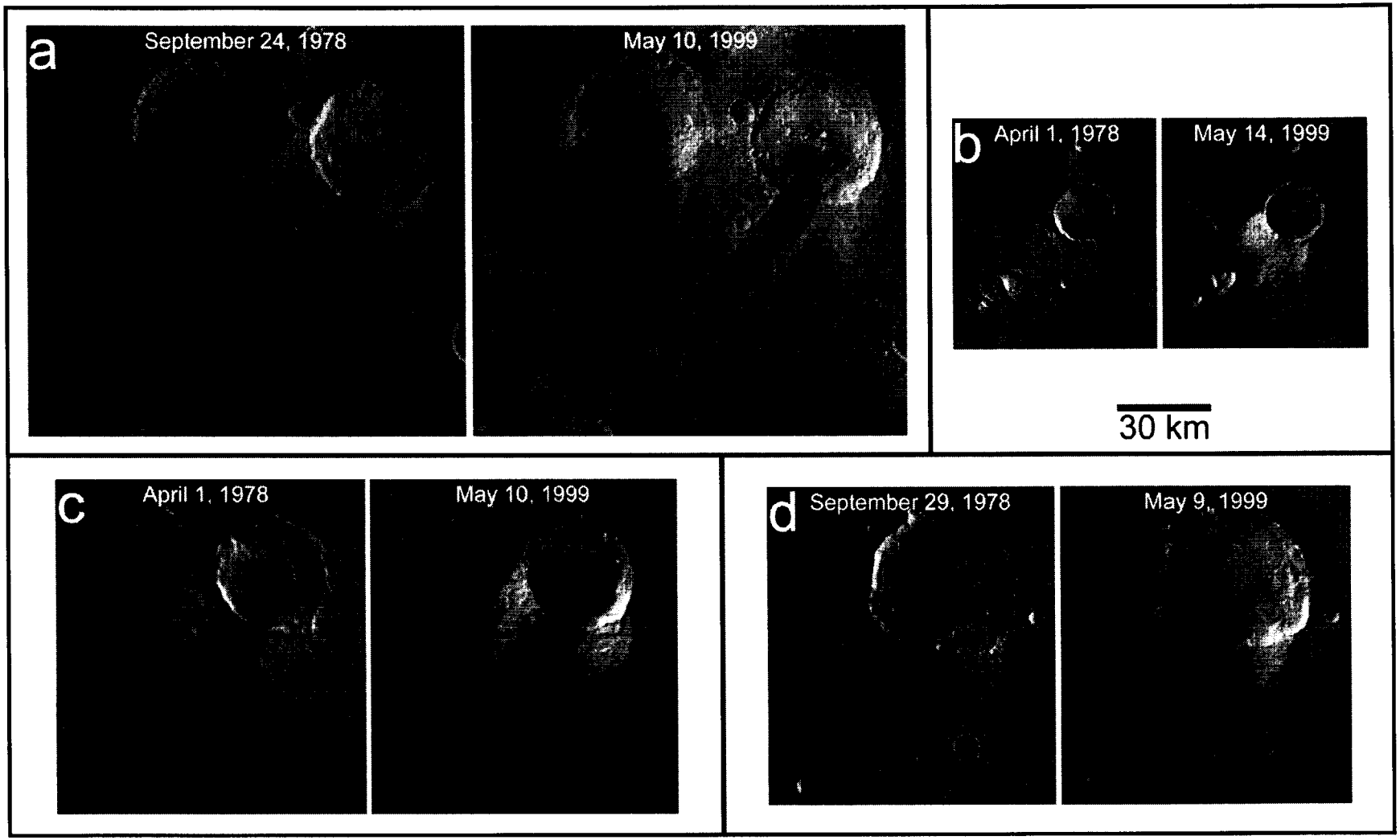
a
September 24, 1978
May 10, 1999
b
April 1, 1978
May 14, 1999
30 km
c
April 1, 1978
May 10, 1999
d
September 29, 1978
May 9, 1999

Figure 20

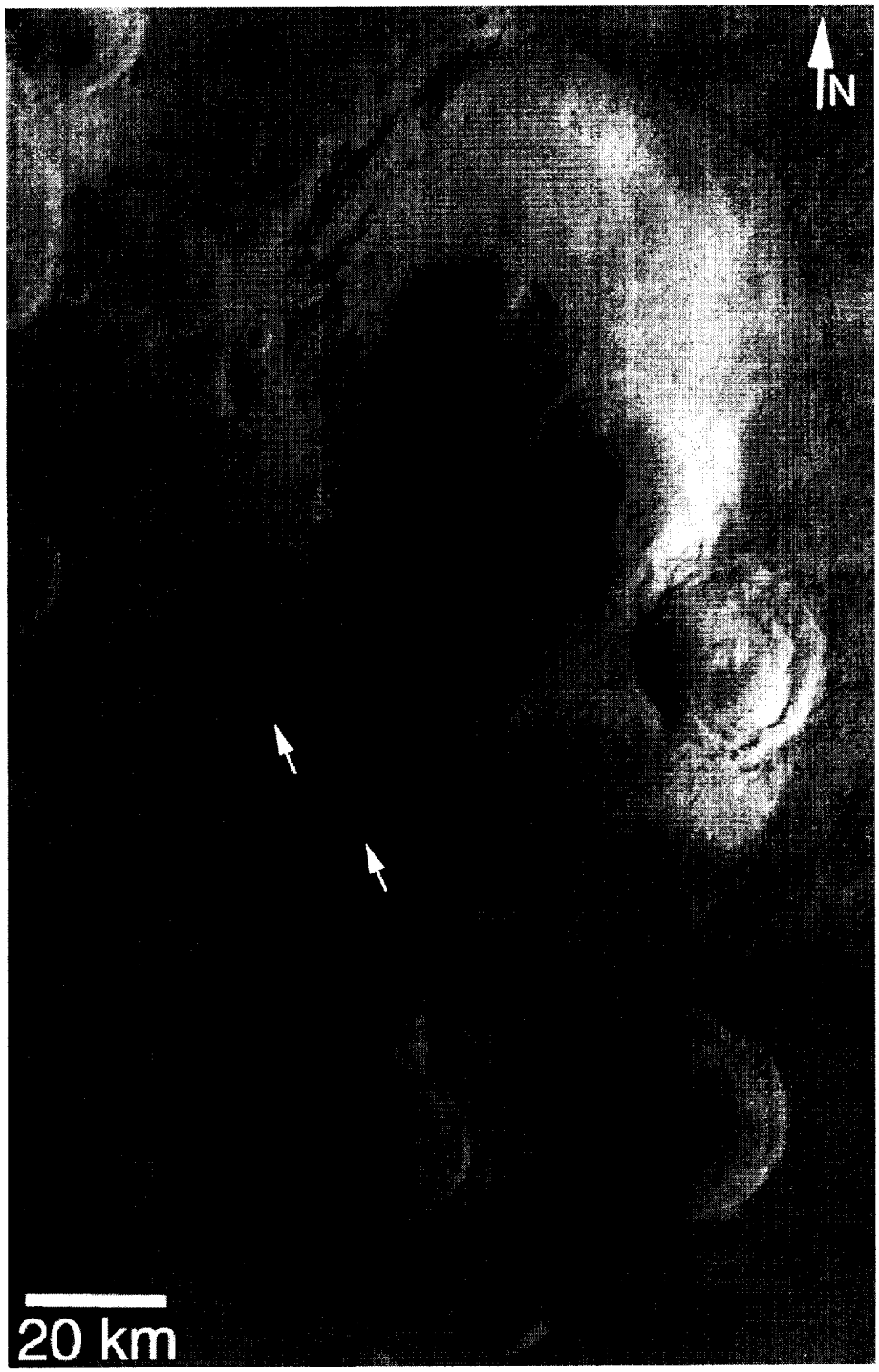

Figure 21

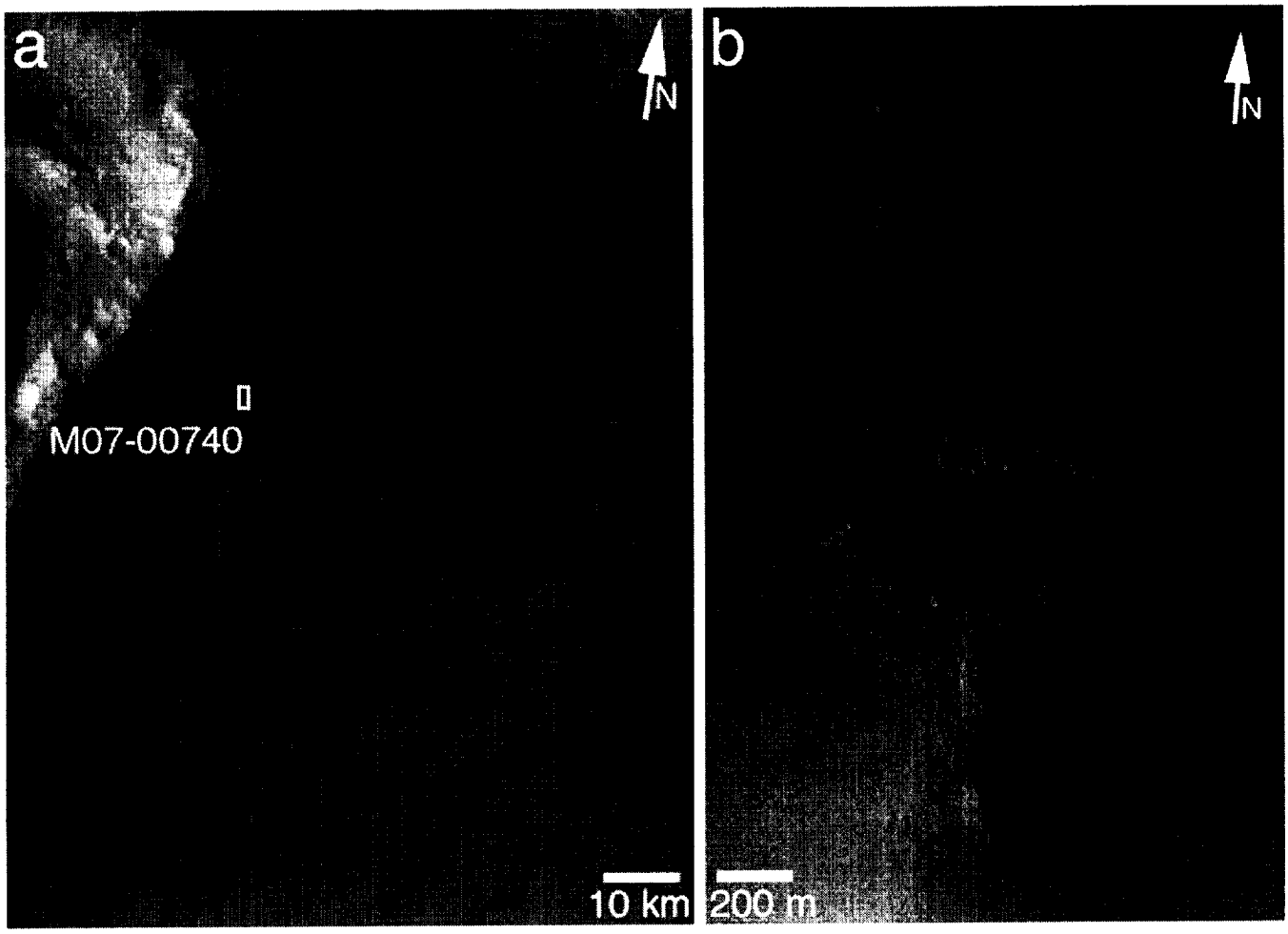

Figure 22

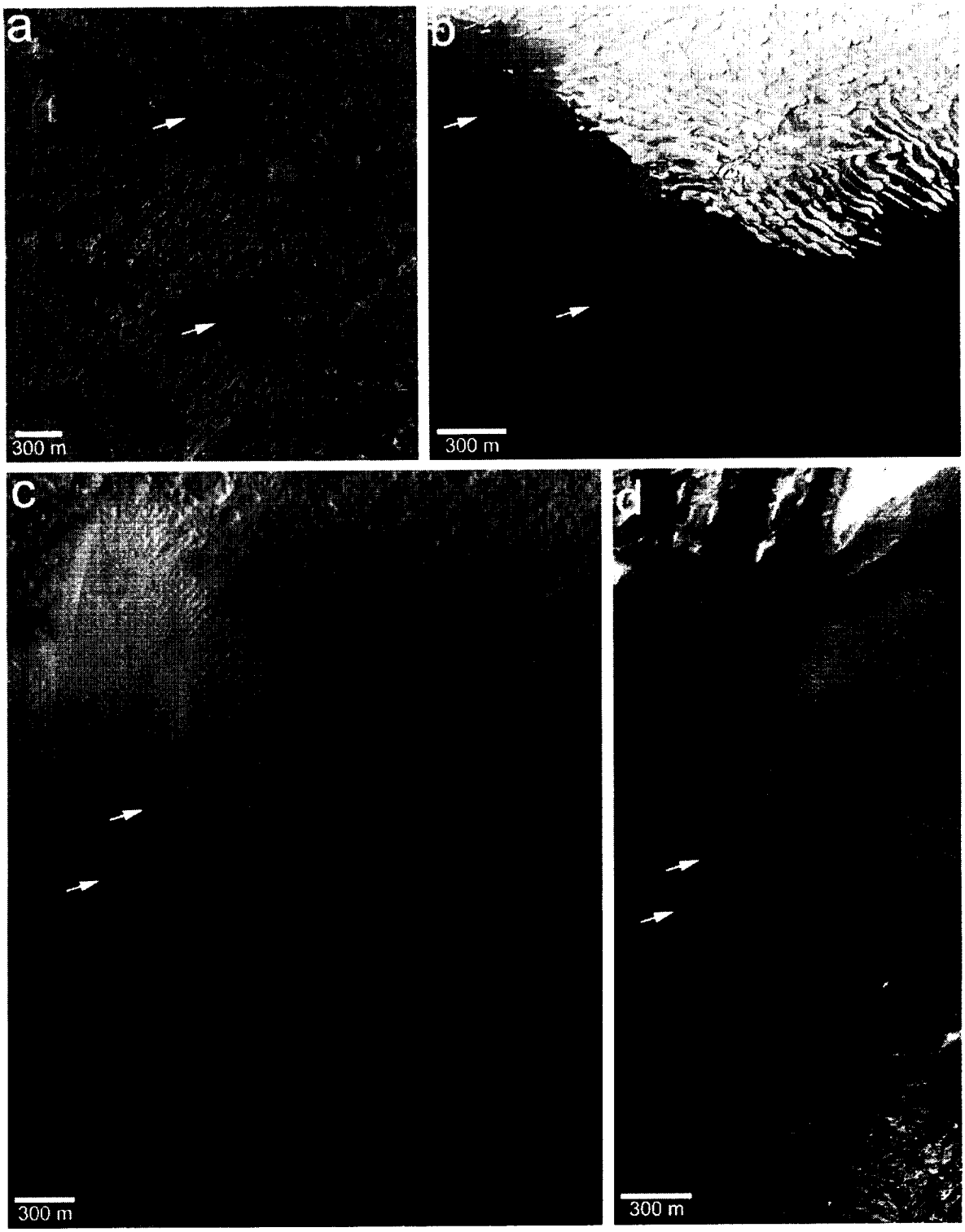

Figure 23

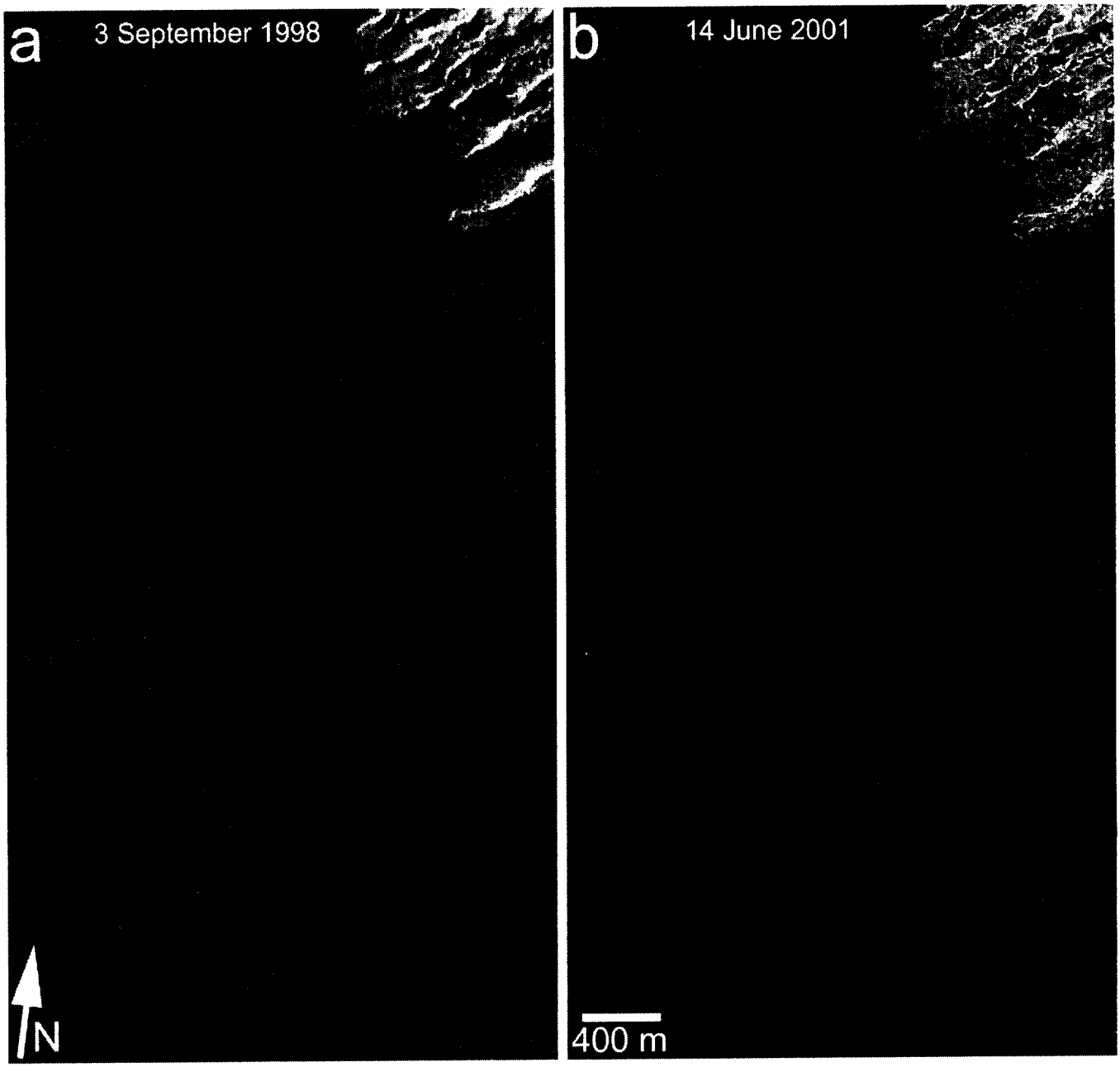

Figure 24